SEMMELWEIS EGYETEM

DOKTORI ISKOLA

Ph.D. értekezések

3137.

MÓZNER ORSOLYA

Patobiokémia

című program

Programvezető: Dr. Csala Miklós, egyetemi tanár

Témavezető: Dr. Sarkadi Balázs, kutatóprofesszor

EXAMINATION OF HUMAN MEMBRANE PROTEINS IN DISEASES- APPLICATION OF MOLECULAR CELL BIOLOGY TO STUDY THE SARS-COV-2 SPIKE PROTEIN

PhD thesis

Orsolya Mózner

Semmelweis University Doctoral School
Molecular Medicine Division

Supervisor: Balázs Sarkadi, MD, DSc

Official reviewers: Viola Pomozi, PhD
                      Balázs Enyedi, MD, PhD

Head of the Complex Examination Committee:
                    Péter Várnai, MD, DSc

Members of the Complex Examination Committee:
                    András Váradi, DSc
                    Balázs Enyedi, MD, PhD

Budapest
2025

Table of Contents

List of Abbreviations

ABC	ATP-binding cassette
ATA	aurintricarboxylic acid
BBB	blood-brain barrier
BCRP	breast cancer resistance protein
CNS	central nervous system
cryo-EM	cryo-electron microscopy
ELISA	enzyme-linked immunosorbent assay
EMA	European Medicines Agency
Fab	Fragment antigen-binding
FDA	United States Food and Drug Administration
GATA-1	GATA-binding factor 1
GWA	genome-wide association
GWAS	genome-wide association studies
MXR	mitoxantrone resistance protein
PMCA4b	plasma membrane Ca2+ ATPase 4b
RBC	red blood cell
RBD	receptor binding domain
RUSH	retention using selective hooks
SBP	streptavidin-binding peptide
SNP	single nucleotide polymorphism
VOC	variant of concern
WHO	World Health Organization

1   Introduction

Membrane proteins are major components of cellular life, responsible for a wide range of functions that are essential for the survival and protection of living cells. From facilitating communication between the intracellular and extracellular spaces to the driving essential metabolic pathways, the roles of these proteins are diverse and critical.

Membrane proteins are characterized by their location within the cell membranes, serving as gatekeepers and mediators in various biological processes. A broad classification of membrane proteins is based on their position in the cell membrane: integral proteins are embedded within the lipid bilayer; peripheral proteins are attached to the inner or the outer surface of the membrane.

These proteins play important roles in a range of biological functions including signal transduction, cellular adhesion, and the transport of substances across cellular barriers. Membrane proteins can act as neurotransmitters, hormones, they can have a function in energy transduction and cell communication.

The dysfunction or altered expression, regulation of human membrane proteins is often linked to diseases, making them important therapeutic targets. For example, changes in the function or expression of membrane proteins can lead to conditions such as cystic fibrosis, Alzheimer's disease, and various cancers.

1.1   Characterization of human membrane proteins

Studying human membrane proteins has always been challenging, they often require specific lipid environments to function, and their structural characterization has always lagged behind that of soluble human proteins due to several limitations. For normal function, they often require glycosylation patterns specific to mammals, post-translational modifications and lipid compositions of the membranes specific to mammals or even more specifically, the human tissues they are expressed in. Widely used and cost-effective systems, such as bacterial or fungal expression systems are often not optimal to express and study human membrane proteins. Recent advances in cryo-electron microscopy and new solutions helped to resolve membrane protein structures better than before[1]. Still, to understand the function of a human membrane protein, adequate, and sometimes complex biological models are required.

1.2 Mutations in membrane proteins

Although learning the physiological function of several human membrane proteins has been successful over the past few decades, it is still a big challenge to predict the effect of mutations in these proteins. Several clinically relevant mutations that lead to severely altered protein function in membrane proteins are known, but there are also many mutations with uncovered effects. With personalized approaches becoming better and more available in medicine, it is important to characterize the consequences of variants in key proteins. Mutations or variants in membrane proteins could lead to diseases or altered cellular processes, they can also have a role in complex mechanisms such as altered response to drug treatments, indirectly causing early onset of diseases, or even protecting against specific conditions or illnesses.

1.3 Uncovering the role of genetic alterations in membrane proteins

As genome-wide genetic analysis becomes more affordable, knowing the effect of specific mutations in genes, including important biomarkers such as membrane proteins, can pose big advantages in patient treatments. The analysis of huge datasets of genetic and patient data gives a great opportunity for researchers to uncover new important biomarkers of diseases in genome-wide association studies. While finding these markers is the first step, the biology behind the association should be uncovered before the knowledge can be translated to the clinic. Understanding the effects of variants in key proteins brings us closer to understanding the normal and dysfunctional cellular processes that these markers are involved in.

1.4 Introduction of the membrane proteins studied in this research work

1.4.1 The ABCG2 multidrug transporter and its variants

ABCG2 is a multidrug transporter of the ABC (ATP-binding cassette) transporter superfamily. ABCG2 has been identified as BCRP, or breast cancer resistance protein in a multidrug resistant human breast cancer cell line in 1998 [2]. It was also cloned and named by two other groups of researchers as MXR (mitoxantrone resistance protein) [3] and as ABC protein expressed in the placenta[4]. Since then, several tissues have been identified to express the protein, and several thousands of endo- and xenobiotic substrates and inhibitors have been identified to interact with ABCG2.

ABCG2 is expressed as a homodimer in the plasma membrane of the cells, where it is responsible for the excretion of a wide range of substances. ABCG2 is expressed in various tissues and tissue barriers in the human body, including the BBB (blood-brain barrier), the intestine, the kidney, the liver, and the placenta [5,6]. ABCG2 is also known to be expressed in a wide variety of stem cells, and in drug-resistant tumor cells, including the "tumor stem cells" or drug-tolerant persister cells [7–9].

ABCG2 is a multidrug transporter, its substrates include endogenous compounds, such as uric acid or estrone sulfate, several drugs like chemotherapeutic agents, antivirals, antibiotics, statins, flavonoids, and a long list of other drugs currently used in medicine. Because of ABCG2's protective role in key physiological barriers and several tissues, the interactions with ABCG2 along with another ABC multidrug transporter, ABCB1 (P-glycoprotein, P-gp) are in the FDA and EMA guidelines [10,11]. Testing potential drug interactions of new drug candidates during drug development and before clinical trials is recommended to evaluate the risks of co-administering ABCG2 or ABCB1 substrates with their inhibitors or competing substrates.

These two ABC transporters are key players in protecting cells from harmful substances, although their substrate specificity and tissue expression differs, there are similarities, and they are expressed together in several tissue barriers, like the BBB; and several drugs interact with both of these transporters. The protein sequence of ABCB1 is very conserved, and naturally occurring variants in healthy individuals affecting the protein coding region are extremely rare, mutations are known to appear in cancer cells. One of the most common variants in ABCB1 is a synonymous SNP, supposed to affect protein expression and function through mRNA translation and protein folding [12]. In contrast, the other key player in multidrug resistance and drug efflux at the blood-brain barrier, ABCG2, has several naturally occurring missense variants that lead to altered expression and function of this protein. The most common variant (rs2231142) results in the Q141K amino acid change, it is so common that around 20% of the global population carries at least one minor allele. It is especially common in the East Asian population, almost half the individuals of East Asian descent carry at least one copy of the minor allele. It has been shown that this variant results in decreased ABCG2 protein levels, have decreased extra-renal urate excretion (through the intestine) and carriers of this variant are more susceptible to gout[13–17]. The FDA guideline separately advises to examine drug

toxicity and interactions in the case of this variant. Because of ABCG2 expression in the blood-brain barrier, together with ABCB1, elevated CNS (central nervous system) exposure to compounds gets great attention [18].

It has also been shown that besides the widely studied and common Q141K variant, multiple rare variants of ABCG2 can lead to decreased protein function and increased gout susceptibility [16].

Although a lot of effort went into developing inhibitors of ABCG2 and ABCB1 to resolve multidrug resistance in cancer, the clinical trials testing these inhibitors failed [19–22].

For the pharma industry, ABCG2 is known as a key player in drug pharmacokinetics, drug absorption and distribution. Drug development strategies often include avoiding ABCG2 substrates and inhibitors to avoid toxicity[23].

Personalized medicine also includes testing for well-known high-impact variants of the ABCG2 transporter. Knowing the consequences of rare variants helps to make personalized decisions. As ABCG2 variants have been linked to a very common disease, gout, there are efforts to identify new, clinically relevant ABCG2 variants among young, early-onset gout patients.[24]

In the plasma membrane of the cells, the functional ABCG2 homodimer has two nucleotide binding domains, ATP binding and hydrolysis give the energy to export substrates [25]. Mutations affecting various positions in the transporter have been shown to lead to altered expression and function of the protein. As a membrane protein, the post-translational fate of the protein is also crucial to get to the plasma membrane, folding, trafficking, and membrane lipid interactions have been studied in the literature. There are still several questions about the checkpoints of these processes.[26]

To study ABCG2 in cellular models in a laboratory setting, fluorescent substrates of the transporter are utilized to measure transport function, antibodies against the extra-and intracellular parts of the protein are available to examine localization and expression levels in various settings[27–29]. The structural model of ABCG2 has been determined via cryo-electron microscopy (cryo-EM), providing valuable insights into the structure-function of this protein[30] (Figure 1). Figure 1 a shows the ABCG2 homodimer with the 5D3 (Fab, Fragment antigen-binding) antibody complex in the inward-facing conformation. Figure 1 b shows the topology color coding, simply shown on Figure 1 c, on figure 1 b, residues previously shown to be crucial are highlighted, the GXXXG motif

is crucial for folding and function of the homodimer [31], while the R482 residue has been widely studied and mutations, like R482G lead to altered substrate-specificity [32]. Q141K is the most common naturally occurring variant of ABCG2, while the C2 motif is a linker region, which was shown to be important in drug transport and ATP binding/hydrolysis [33].
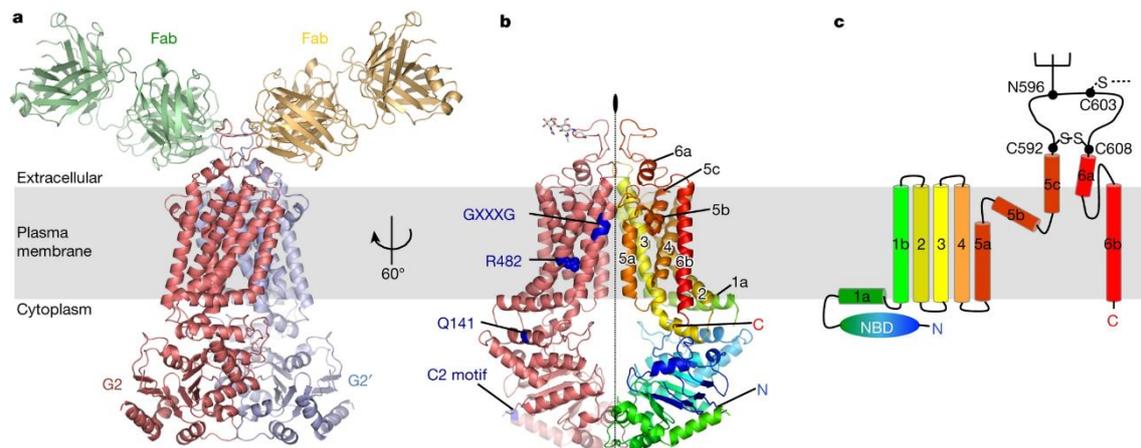
Figure 1. Structural model of the ABCG2 transporter determined via cryo-EM. a, homodimer ABCG2-5D3(Fab) antibody complex. b, ABCG2 structural model without the 5D3-Fab. Right side monomer colored from N-terminal (blue) to C-terminal (red). c, topology of the ABCG2 transmembrane domain structure colored as in b. C592, C608, and C603 cysteines form disulfide bonds. The protein is N-glycosylated on residue N596. Figure source: Taylor, N., et al. [30]

A recent animal study revisits the role of multidrug transporter inhibitors in cancer, by providing a new treatment strategy separating the multidrug transporter inhibitor and the chemotherapeutics to avoid toxicity in healthy tissues[34]. A different research approach has been proposed to focus on the genetic regulation of *ABCG2* transcription and find targets for ABCG2 function through decreasing the produced protein in the cell, preferably tissue-specifically, instead of protein-level inhibition all over the body [35].

1.4.2 The PMCA4b calcium transporter and a haplotype in the *ATP2B4* gene

The plasma membrane Ca^{2+} ATPases (PMCAs, encoded by *ATP2B1-4*) play critical roles in calcium homeostasis, an important process for many physiological functions. There are four isoforms of PMCA, encoded by the genes *ATP2B1* through *ATP2B4*, each responsible for regulating calcium levels within different cell types and tissues [36]. Ca^{2+} ions serve as secondary messengers in diverse cellular functions, including neurotransmission, muscle contraction, and signaling pathways. PMCAs are ATP-dependent, P-type ATPase pumps that export Ca^{2+} from the cytoplasm into the extracellular space, keeping intracellular Ca^{2+} levels low [37]. Each PMCA isoform is activated by Ca^{2+}/calmodulin binding to the autoinhibitory domain, this regulation enhances their activity in response to increases in Ca^{2+} [38].

There are several splice variants of the four isoforms, that allow unique expression patterns and specialized roles in specific tissues. The human plasma membrane Ca^{2+} ATPase isoform 4, splice variant b (PMCA4b), encoded by the *ATP2B4* gene on chromosome 1, plays an important role in cellular calcium regulation in hematopoietic cells such as platelets and erythrocytes. In these cells, maintaining low cytoplasmic calcium levels is crucial to prevent unwanted cell activation and dehydration, which can lead to pathological states. [34]

Beyond its general role in cellular Ca^{2+} regulation, PMCA4b also has implications in disease susceptibility, including malaria. Genome wide association (GWA) studies have indicated that a given set of single nucleotide polymorphisms (SNPs) in the *ATP2B4* gene confers resistance to a severe form of malaria among children. These SNPs have also been linked to reduced malaria severity in pregnant women, protects against malaria-associated maternal anemia, and modulation of cellular dehydration [39,40]. It has been shown that PMCA4b expression on RBCs varies among individuals, and the decrease in PMCA4b expression can be explained by a minor haplotype in the *ATP2B4* gene, this minor haplotype is the same that has been indicated to be protective in malaria infection [41].

Although the exact mechanism connecting PMCA4b to malaria is still under investigation, a potential mechanism was recently proposed. According to this hypothesis, the reduced expression level of the active calcium transporter on RBCs (red blood cells) lead to elevated Ca^{2+} ion levels, which could result in the opening of the Gardos channel, a potassium channel that, when open, causes potassium efflux, water loss, and leads to

erythrocyte dehydration in RBCs [42]. This hypothesized mechanism could result in a less hospitable environment for the malaria-causing *Plasmodium falciparum* [43]. A recent study proposed a potential treatment strategy that involves the inhibition of PMCA4b by aurintricarboxylic acid (ATA) to slow the growth of *P. falciparum* in the RBCs. [44]

The *ATP2B4* gene encoding PMCA4b is subject to regulatory mechanisms that control its expression in erythroid cells. GATA-1 is a key erythroid-specific transcription factor, known to be involved in erythropoiesis, and it has been suggested to be involved in the erythroid-specific regulation of *ATP2B4* [45]. Some of the SNPs in the haplotype associated with susceptibility to a severe form of malaria are in predicted GATA-1 binding sites [46]. In the present work, the molecular background and the exact SNPs of the haplotype were examined to study the erythroid-specific regulation of PMCA4b expression.

1.4.3 The spike protein RBD of the SARS-CoV-2 virus

The SARS-CoV-2 virus, responsible for the COVID-19 pandemic, infects host cells through the interaction of the spike (S) protein with the angiotensin-converting enzyme (ACE2) receptor on the infected cell surface [47]. The spike protein has a trimeric structure, with each monomer composed of two subunits, S1 and S2. The receptor binding domain (RBD) is a crucial part of the S1 subunit of the spike protein, that directly engages the ACE2 receptor, initiating cell entry and subsequent infection. The RBD is a key target for neutralizing antibodies and important point in the design of vaccines and therapeutic interventions [48].

The glycosylation pattern of the spike protein is essential for immune evasion and proper folding in mammalian systems, making them ideal for producing bioactive forms of this protein for research and diagnostics [49,50]. In Figure 2, the spike protein is shown bound to the ACE2 receptor, illustrating the molecular interaction that allows the virus to enter the host cells.
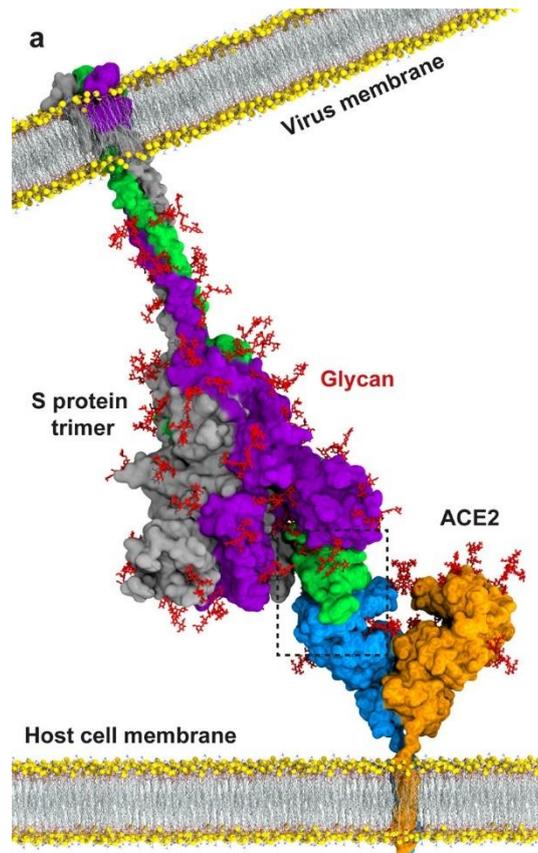
Figure 2. Atomic model of the SARS-CoV-2 spike protein trimer bound to the ACE2 receptor on the host cell membrane. Figure source: Taka E. et al. [51]

Since its initial identification, SARS-CoV-2 has undergone significant mutations, leading to the emergence of multiple variants with altered infection and immune escape profiles. The Omicron variant (B.1.1.529) was first detected and named variant of concern in late 2021 by the WHO (World Health Organization). Signature Omicron mutations are found in most of the Omicron lineages, but there are big differences between the BA.1, the BA.2.75, the XBB.1.5 and the EG.5.1 lineages in mutations in the S1 subunit of the spike protein, especially within the RBD. [52] These sub-variant specific mutations ask for constant reassessment of immune protection and diagnostic methods to accurately monitor immunity and predict vaccine efficacy worldwide.

Immunity after infection or vaccination protects against future infections and can prevent severe symptoms during future infections [53,54]. This protection is typically transient and varies among individuals and against different virus variants. Immunity to SARS-CoV-2, particularly through neutralizing antibodies targeting the spike protein, is crucial for preventing severe disease [55]. In addition, immune escape variants emerged and are

causing concern to this day. Several variants acquired antibody-escaping mutations, that often affect the receptor binding domain of the SARS-CoV-2 spike protein. Protective immunity against the infection is crucial to be assessed for identifying high-risk patients without protective immunity and the efficacy of vaccines. As emerging variants can have altered infection properties and they often escape immune response, it is important to adapt our testing systems and methods in a variant-specific manner. [56] Most tests assessing immunity in the clinic test for antibody levels against the SARS-CoV-2 spike protein. These calibrated ELISA tests give an estimate of antibody levels in the sera of the patients against specific variants. New variants often escape these antibodies against previous variants, and it has been shown that protective immunity against SARS-CoV-2 is a complex mechanism, with several important factors other than antibodies [57,58]. T-cellular immunity plays a crucial role in the protective immune response against SARS-CoV-2 infection [59,60]. Unfortunately, assessing T-cellular immune response is a complex and costly process. Vaccines are updated to include and immunize against the most recent variants, testing the efficacy of recent vaccines and previous infections against the current variants is a constant challenge. [56]

2   Objectives

In my PhD research, I aimed to study the effects of naturally occurring variants affecting the ABCG2 and PMCA4b human membrane proteins. Under the Cooperative Doctoral Program, I aimed to apply the techniques I used to examine membrane proteins to generate a cell line which can be suitable to produce the SARS-CoV-2 spike RBD protein for diagnostic purposes.

My aims were to

> **Explore the consequences of the K360del (rs750972998) ABCG2 variant**: Investigate the impact of the variant on protein expression and function, and the role of the unstructured cytoplasmic loop affected by this variant.

> **Examine the effect of a haplotype in a regulatory region of the *ATP2B4* gene**: Study the effect of a haplotype in a supposed regulatory region of the *ATP2B4* gene encoding the PMCA4b calcium transporter protein.

> **Generate a stable HEK293 suspension cell line**: Develop a stable HEK293 suspension cell line to produce the SARS-CoV-2 spike and spike RBD proteins secreted into the serum-free cell culture media.

> **Measure serum antibody levels against variants of the SARS-CoV-2 spike RBD in an ELISA assay:** Produce RBD proteins according to the altered sequence of newly emerging SARS-CoV-2 variants and use them in an ELISA to evaluate the anti-spike-RBD antibody levels of vaccinated individuals and COVID-19 patients.

The research process included the identification of the best molecular biological and cellular biological methods to examine the effects of clinically relevant variants. The production of the RBD protein was achieved using the same stable cell line generation method applied in the other experiments.

3 Methods

3.1 Vector constructs

The p10-[expressed protein coding gene]-IRES2-GFP transposon vector was used in experiments that involved the expression of untagged ABCG2 variants and the tagged spike and spike-RBD. Mutations were introduced in the ABCG2 and spike-RBD coding sequence by mutagenesis PCR and cassette change. The spike and spike-RBD expression cassette was cloned from the expression vector described in Amanat et al. [61] containing the N-terminal spike secretion signal for protein expression excreted into the culture media, and a C-terminal His-tag for downstream processing. All vector sequences were checked by Sanger sequencing. The p10 vector is a transposon coding vector, for stable cell line generation by the transposon–transposase method, it was used together with the SB100 Sleeping Beauty transposase-coding vector, in 9:1 molar ratio (p10:SB100 vector) [62]. In experiments examining transient expression after 2 days, it was used without the transposase vector.

For the dynamic trafficking experiments, RUSH vectors containing N- terminally tagged ABCG2 variants and an endoplasmic reticulum (ER) hook were used as described by Bartos and Homolya 2021 [63]. Mutations were introduced into these plasmids from the above-mentioned templates, by replacing the WT-ABCG2 coding sequence with the examined ABCG2 mutant coding sequences. The mutant ABCG2 coding new plasmids were checked by Sanger sequencing.

In the *ATP2B4* gene, four regions affected by SNPs in the haplotype were examined: the H1st, the PR2, the H1.1 and the H1.2. (See Figure 8; and [64]). These sequences were amplified from genotyped genomic DNA samples (from WT or homozygous haplotype-carriers) and inserted into the pGL4-Firefly luciferase plasmid, which did not contain a promoter, so the promoter activity of the inserted sequences could be tested by measuring the luciferase activity in the transfected cells. The pRL-TK-Renilla vector was used as a control in the experiments (Promega Dual-Luciferase Reporter Assay System, Promega Corporation, Madison, WI, USA, cat. E1910).

3.2 Cell culture and transfection

HEK293H (human embryonic kidney cell line; Gibco, Thermo Fisher Scientific, Waltham, MA USA cat. CVCL_6643), HeLa (human cervical adenocarcinoma cell line;

Manassas VA, USA cat. CCL-2), MDCKII (epithelial cell line from canine kidney; ECACC 00062107) adherent cell lines and K562 (human chronic myelogenous leukemia cell line; ATCC CCL-243) and HEL.92.1.7 (human erythroleukemia cell line; ATCC TIB-180) suspension cell lines were used in the experiments. HEK293, HeLa and MDCKII cells were grown in DMEM/high glucose/GlutaMAX medium (Gibco, Thermo Fisher Scientific, Waltham, MA USA cat. 10569010), while K562 cells in IMDM/GlutaMax (Gibco, Thermo Fisher Scientific, Waltham, MA USA cat. 31980030), HEL cells in RPMI-1640/GlutaMax (Gibco, Thermo Fisher Scientific, Waltham, MA USA cat. 61870010) cell culture medium, all media completed with 10% FBS (Gibco, Thermo Fisher Scientific, Waltham, MA USA cat. 1640071) and 1% Penicillin-Streptomycin (Gibco, Thermo Fisher Scientific, Waltham, MA USA cat. 15070063) at 37 °C (5% CO2). TrypLE Express Enzyme (Gibco, Thermo Fisher Scientific, Waltham, MA USA, cat. 12605010) dissociation reagent was used for 5 minutes in the case of adherent cell lines. Transfection of HEK293 and HeLa cells was carried out with Lipofectamine 2000 (Invitrogen, Thermo Fisher Scientific, Waltham, MA USA cat. 11668019) in Opti-MEM medium (Gibco, Thermo Fisher Scientific, Waltham, MA USA cat. 31985070), (1 µL transfection reagent + 500 ng total plasmid DNA). Transfection of K562 and HEL cell lines was carried out with the Mirus TransIT 2020 (Mirus Bio, Madison, WI, USA, cat. MIR5404) transfection reagent. The transfection reagent and the plasmid (0.2 µL transfection reagent + 100 ng total plasmid DNA) were diluted in Opti-MEM medium.

HEK293 cells expressing the spike and spike-RBD were converted to serum-free culturing by transferring the cells from the 10% FBS DMEM to the FreeStyle293 serum-free expression medium (Gibco, Thermo Fisher Scientific, Waltham, MA USA cat. 12338026).

For cycloheximide treatment in ABCG2 variant experiments, 20 µg/mL final CHX concentration in completed DMEM/high glucose/GlutaMAX was used. Normal growth medium was replaced by CHX medium for 1 or 4 h. We used a 100 mg/mL CHX in DMSO stock solution (Sigma Aldrich, Burlington, MA USA cat. C4859).

3.3   Stable cell line generation

The stable cell lines were generated by the Sleeping Beauty transposon-transposase system. The SB100 Sleeping Beauty transposase inserted the transposon sequence coded on the p10 vector. Successfully transfected cells were sorted using BD FACS Aria III

based on green fluorescence and further cultured. 2 weeks later, cells still showing fluorescence were sorted, these cells contained the transposon sequence integrated randomly into their genome. The p10 transposon vector contained the above-described CAG-[ABCG2 or spike]-IRES2-EGFP sequence, which allowed for the overexpression of the ABCG2 or the spike/spike-RBD proteins. The CAG-[ABCG2 or spike]-IRES2-EGFP sequence allowed for a fluorescent marker that was expressed in stable cells from the same mRNA but without the tagging of the ABCG2 or the spike protein. Different ABCG2 variant-expressing cell lines were sorted for similar GFP fluorescence.

Spike and spike-RBD expressing cell lines were single-cell sorted on 96-well plates and further cultured, only cells showing high GFP were selected, and further analyzed based on their spike protein expression. Cell lines derived from one single cell were characterized and those showing the highest yield were selected and later converted to serum-free culture medium as described above.

In the case of the MDCKII cells, cells were sorted once, 4 days after transfection and further cultured, which resulted in a mixed culture, where several cells were stably expressing the ABCG2 variant; although there were negative cells in this culture, it was suitable for future analysis to examine the localization of ABCG2 in the polarized MDCKII cells.

3.4   Dual-luciferase assay to measure promoter activity

The dual-luciferase reporter system was used for 96-well cultured HEK293, HEL, K562 confluent cells. Results were read by the VictorX3 Multilabel Plate Reader. Reagents were added on 96-well white plates to the cell lysates manually, right before reading the signals, one by one. Firefly luminescence was read first, then Renilla luminescence was read after the addition of the stop reagent. At least two biological and two technical parallel experiments were carried out in all cases. Firefly/Renilla luminescence data were normalized to HEK WT results, in experiments involving GATA-1 coexpression, to HEK-WT without GATA1 overexpression. Results were analyzed by two-tailed unpaired Student's t-tests.

3.5   RNA isolation, cDNA PCR

RNA isolation was performed by the PureLink RNA Mini Kit (Invitrogen PureLink^{TM} RNA Mini Kit, Thermo Fisher Scientific, Waltham, MA, USA, cat. 121183020), 1×10^6

cells to examine GATA-1 mRNA expression in the HEK293, HEL, and K562 cell lines. GATA1 specific primers were used to amplify GATA1 cDNA in a PCR reaction with Phusion High Fidelity DNA polymerase. (New England Biolabs, Ipswich, MA, USA, cat. M0530S)

3.6 Culturing of HEK293 cell lines that stably produce the RBD protein and isolation of the protein from the culture media

The cell lines were grown in suspension, and the cultures were shaken (100 rpm) in serum-free media (FreeStyle 293 Expression Medium, Gibco, Cat. 12338018, Waltham, MA, USA) at 37 °C, 5% CO2. The RBD protein was isolated and purified by nickel ion affinity chromatography (ÄKTA pureTM, GE Healthcare, Chicago, IL, USA). Elution was performed by 200 mM imidazole, pH 7.4. Concentration and buffer exchange to PBS were performed by 30 kDa filters (Vivacell 100, Sartorious, Göttingen, Germany). The protein product size and purity were examined by SDS-polyacrylamide gel electrophoreses; concentration was estimated by UV–vis spectrophotometry at 280 nm.

3.7 Hoechst33342 uptake measurements in ABCG2-expressing cells

To examine the function of different ABCG2 variants, Hoechst33342 dye uptake measurements on live cells expressing the ABCG2 variants were performed. Hoechst33342 is a fluorescent dye and substrate of the ABCG2 transporter, if the transporter functions well, it exports the dye from the cells. Ko143 is a specific inhibitor of the ABCG2 transporter, when used in low amounts as in the experiments.

48 hours after transfection, trypsinized cells were incubated and gently shaken for 20 min at 37 °C in HPMI buffer (20 mM HEPES, 132 mM NaCl, 3.5 mM KCl, 0.5 mM MgCl2, 5 mM glucose, 1 mMCaCl2, pH 7.4) with 1 μM Hoechst33342 (Thermo Fisher Scientific, Waltham, MA USA Thermo Fisher Scientific, cat. H1399) after preincubation for 5 min with the presence or absence of 1 μM of the Ko143 (Tocris Bioscience, Bristol UK cat. 3241) ABCG2 inhibitor. Following incubation with the dye, cells were put on ice until measurement. Hoechst33342 fluorescence of the cells was measured by the Attune NxT Cytometer (Thermo Fisher Scientific, Waltham, MA USA Thermo Fisher Scientific). GFP fluorescence was detected in the BL1, while Hoechst33342 fluorescence was detected in the VL1 detector. For data analysis, the Attune NxT Cytometer Software v3.1.2 was used. MAF (multidrug resistance activity factor) values [65] were calculated from the results

the following way: MAF = $(F_{(inh)} - F_{(no\ inh)})/F_{(inh)}$, where $F_{(inh)}$ is the median of Hoechst fluorescence of the cells with the inhibitor, while $F_{(no\ inh)}$ is the fluorescence of the cells without the inhibitor. When comparing these results to cell surface expression levels, the activity factor was divided by cell surface expression levels, measured by flow cytometry after ABCG2-specific 5D3 antibody labeling.

3.8 ABCG2 plasma membrane expression measurement

Cell surface expression of ABCG2 was determined in the transfected HEK293 and HeLa cells 48 h after transfection. Trypsinized cells ($1*10^6$/tube) were incubated in small volumes (100 μL) and gently shaken for 40 min at 37 °C in 0.5% BSA/PBS with 1 μM Ko143 (Tocris Bioscience, Bristol UK cat. 3241) and the ABCG2-specific 5D3 mouse monoclonal antibody (gift of Bryan Sorrentino, Division of Experimental Hematology, Department of Hematology/Oncology, St. Jude Children's Research Hospital). Ko143 was added to the samples because it has been shown to help the conformation-sensitive 5D3 antibody recognition. Cells were washed twice with 2 mL PBS. After washing, the cells were centrifuged and the supernatant discarded, then incubated for 30 min at 37 °C with the secondary antibody (goat anti-mouse IgG2b Alexa Fluor 647, cat. A-21242, Invitrogen, Thermo Fisher Scientific, Waltham, MA USA) in 0.5% BSA/PBS. Cells were washed again with 2 mL PBS. Measurements were performed in the Attune NxT Cytometer (Thermo Fisher Scientific, Waltham, MA USA) using the RL1 detector. For data analysis, the Attune NxT Cytometer Software v3.1.2 was used.

3.9 Western blotting

Protein samples were isolated from the cells in TE sample buffer (0.1 M TRIS-phosphate, 4% SDS, 4 mM Na- EDTA, 40% glycerol, 0.04% β-mercaptoethanol and 0.04% bromophenol blue) for Western blot experiments, or as described in the SARS-CoV-2 RBD purification. Equal amounts of protein samples were loaded on 10% acrylamide gels, PVDF membrane was used for blotting. For detecting the examined proteins in the ABCG2 project, the anti-ABCG2 (BXP-21, Abcam, Cambridge, UK, cat. ab3380) and anti-GFP (Abcam, Cambridge, UK, cat. ab290) monoclonal antibodies were used, in the PMCA4b project the anti-GATA1 (Abcam ab181544) rabbit monoclonal and anti-β-actin (Sigma, cat. A1978) mouse monoclonal, in the spike-RBD detection, the anti-His (Sig-Aldrich Cat. H1029, St. Louis, MO, USA) and anti-RBD (Invitrogen cat. MA5-38033,

Thermo Fisher Scientific, Waltham, MA, USA) primary antibodies; goat anti-mouse IgG (H + L) HRP conjugate (Abcam ab97023) and goat anti-rabbit IgG (H + L) HRP conjugate (Abcam ab6721) secondary antibodies and Pierce™ ECL Western Blotting Substrate (BioRadCat.1705061, Hercules, CA, USA) were used. Luminescence was detected with the BioRad ChemiDoc MPImaging System. Densitometry analysis was performed by ImageJ software v1.42q.

3.10 Immunostaining and confocal imaging of MDCKII cells

MDCKII cells were cultured under polarizing conditions on Corning Costar 24-well transwell plates with 24-well transwell insert polyester membranes (Corning Inc., Corning, NY, USA, cat. 3470) for 5 days. The membrane was cut from the transwell and transferred to microscope slides after immunostaining. For immunostaining, cells on the transwell were gently washed with PBS and fixed with 4% paraformaldehyde in PBS for 5 min at room temperature, followed by permeabilization in methanol for 5 min on ice. After washing, samples were blocked for 1 h at room temperature with 2% BSA, 1% fish gelatin, 0.1% Triton-X 100, 5% goat serum in PBS (blocking buffer), and all antibodies were diluted in blocking buffer in the following steps. Samples were incubated for 1 h at room temperature with primary ABCG2 antibody (mouse, Bxp-21 1:200, Abcam, Cambridge, UK, cat. Ab3380) and Na,K-ATPase antibody (chicken, 1:500, Abcam, Cambridge, UK, ab353),which was used as a basolateral marker. After washing with PBS, cells were incubated for1 hat room temperature with the secondary antibodies (1:250, Alexa Fluor 647-conjugated goat anti-chicken, Thermo Fisher Scientific, Waltham, MA, USA, cat. A-21449 and Alexa Fluor 568 goat anti-mouse Thermo Fisher Scientific, Waltham, MA, USA, cat. A-11004). Immunostaining was performed in the transwell, and for the confocal microscopy, the membrane was cut from the insert and transferred to microscope slides. Cells were imaged by the Zeiss LSM 710 confocal laser scanning microscope, and images were processed with ZEN 2012 software, blue edition.

3.11 Confocal microscopy imaging and kinetic analysis of ABCG2 trafficking

To analyze the cellular trafficking of the ABCG2 variants in detail, the dynamic RUSH system was used [63,66]. Briefly, the ABCG2 variant tagged with streptavidin-binding peptide (SBP) and GFP, and an ER-resident hook protein (the invariant chain of major histocompatibility complex (MHC) class II) tagged with streptavidin, were transiently co-

expressed in HeLa cells. ABCG2 was retained in the ER. To release ABCG2 from the ER, 100 µM biotin was added to the cells, together with 5D3-Alexa Fluor 647 conjugated antibody (1 µg/mL, Novus Biologicals, Littleton, CO, USA, cat. FAB995R) together with 1 µM of the ABCG2 inhibitor KO143 (Sigma-Aldrich, Burlington, MA, USA, cat. K2144). This antibody recognizes the extracellular part of the ABCG2 protein in a conformation-specific manner [67].After 1, 2, or 4 h incubation, the samples were gently washed with PBS, fixed with 1% PFA for 5 min at room temperature and washed again 3 times with PBS. For time point zero, no biotin was used. The cells were imaged by confocal microscopy as specified above. For each condition, six fields of view containing 15-20 transfected cells were acquired in 3-4 biological parallels. The 3 variants examined were the WT-ABCG2, K360del and the K360A variants.

For the kinetic analysis, the localization-based colocalization coefficients (CC) of red vs. green fluorescence (5D3 ABCG2 labeling vs. the GFP fluorescence of the ABCG2 tag) were derived from the images at each condition using the ZEN2012 software. The time courses were then fitted with a sigmoidal function using the least square method as described in Bartos and Homolya 2021[63]. The kinetic parameters, such as the initial values (CC_0), the limits of the function (CC_{inf}) and the time constants (k) were determined. For statistics, Student's t test was used. Differences were considered significant when $p < 0.05$.

3.12 ELISA method used to determine antibodies against the SARS-CoV-2 RBD from human serum samples

We have determined the specific recognition of the purified proteins in their native state by the anti-RBD monoclonal primary (Abcam ab273074 and Invitrogen 703959) and HRP-conjugated secondary antibody (Abcam ab6724, Cambridge, UK). In order to calibrate the indirect ELISA allowing for detection of RBD-specific IgG antibodies in human sera, we have applied various concentrations of the purified RBD protein and pre-COVID-19 sera, as well as sera of non-vaccinated or fully vaccinated volunteer donors. We found that 0.4 µg RBD protein and 500× dilution of the sera provided well-measurable interaction in all vaccinated donors and minimum signal in the non-vaccinated donor. In this ELISA, we used High Binding 96-well ELISA microplates (Corning Inc. Cat. 9018, Corning, NY, USA) and the tested amount of RBD in 100 µL PBS incubated overnight (16h) at 4 °C. The samples were blocked by 0.5% BSA/PBS for one hour at room

temperature, then washed 3× in PBS-0.1%Tween 20. The commercially available anti-RBD monoclonal antibody (Abcam, cat. ab273074 and Invitrogen Cat.703959) was applied in 1:2000 dilution in 0.5% BSA/PBS for one hour at room temperature, washed 3 times with PBS-0.1% Tween 20. The secondary antibody (anti-rabbit HRP, Abcam, cat. ab6721) was applied in a dilution of 1:20000 in 0.5% BSA/PBS for 45 min, washed 3 times in PBS-0.1% Tween 20, and then we used TMB substrate (Thermo Scientific cat. 34021, Waltham, MA, USA) for quantification. The absorbance was read in a VictorX multilabel plate reader at 660 nm after 10 min; (A unit) was calculated by multiplying the absorbance by 1000.

In the indirect ELISA designed to measure SARS-CoV-2 spike IgG titers from human sera, High Binding 96-well ELISA microplates (Corning Cat. 9018, Corning, NY, USA) coated with 0.5 µg RBD in 100 µL PBS per well were used. Coating was performed overnight (16 h) at 4 °C. For blocking and the dilution of sera and antibodies, we used 0.5% BSA/PBS (Bovine Serum Albumin Sigma-Aldrich Cat.A7030, PBS Gibco Cat.20012027). After 1 h blocking at room temperature, plates were washed 3 times with 0.1% Tween-20/PBS and incubated with 100 µL 1000× diluted sera in 0.5% BSA/PBS at room temperature for 1 h, washed 3 times again, and incubated for 45 min with HRP-conjugated anti-human IgG secondary antibody (Invitrogen Cat.A18805). After washing 3 times, 100 µL TMB substrate solution (TMB Substrate Kit, Thermo ScientificTM Cat. 34021 Waltham, MA, USA) per well was added; blue color reaction could be measured at 660 nm, 5 min after adding the TMB substrate; the reaction was stopped by the addition of 100 µL 0.16 M H_2SO_4 solution per well. The absorbance at 450 nm was measured by a Perkin Elmer Victor X3 multilabel plate reader spectrophotometer; (A unit) was calculated by multiplying the observed absorbance at 450 nm by 1000. For example, if the observed absorbance of a given sample was 0.5, the "A unit" in the results is 500.

Each serum sample was measured in two parallels, and the average of the two measurements was calculated. Control wells without serum in the case of all three types of RBDs and controls with all used diluted serum samples with no coating antigen were used in all experiments. Sample preparation: fingertip blood samples were immediately centrifuged in polypropylene microcentrifuge tubes at 1000× g for 5 min, and the serum was collected from the top into a sterile new tube. Samples were then frozen and stored at −20 °C for short term and at −80 °C for long term. Clinical sera samples prepared in

the hospital were stored at −80 °C. Visualization of the results was performed using GraphPad Prism 8 Software (GraphPad Software, Boston, MA, USA).

3.13 Statistical Analysis and Graphs

All experiments were performed with at least two biological replicates. GraphPad Prism 8.0.2 was used for statistical analysis and visualization of the results. ABCG2 cell surface expression levels (5D3), Hoechst dye accumulation results and Western blot quantification results and variant-specific average antibody levels were analyzed by one-way ANOVA, and Dunnett's multiple comparison test (95% confidence interval) was performed to compare results to the WT-ABCG2 results. Columns marked with a star showed significant difference (adjusted p value < 0.05) compared to the WT-ABCG2 results.

In the case of the PMCA4b and *ATP2B4* related results, mean values were compared via t-test and significant differences are marked with one, two or three stars *(* p<0.05, ** p < 0.01, *** p < 0.001).* The statistical analysis used is addressed in the Results section Figure descriptions.

4 Results

4.1 Examination of cytoplasmic loop variants of the ABCG2 multidrug transporter

I have examined the structurally unresolved cytoplasmic region in the ABCG2 transporter, a loop of amino acids from 354 to 367 (see this on an ABCG2 structure with this loop appearing as modeled on Figure 3(a) as published in our paper [68]). This loop region contains four neighboring lysines (K357-K358-K359-K360), in the case of the K360del naturally occurring variant, one of the four lysines is deleted. This loop also contains a potentially phosphorylated threonine (T362) residue, which was reported to be phosphorylated and to have an important regulatory role. [69,70]

The examined variants studied in the experiments are K360del, K360A, K359A, K358A, K357A, double mutant K357A, K360A, a variant where all the four lysines were replaced with alanines (K357- K360A) and two variants that affect the T362 supposed phosphorylation site, T362A and a phosphorylation-mimicking T362E (Figure 3(b)).
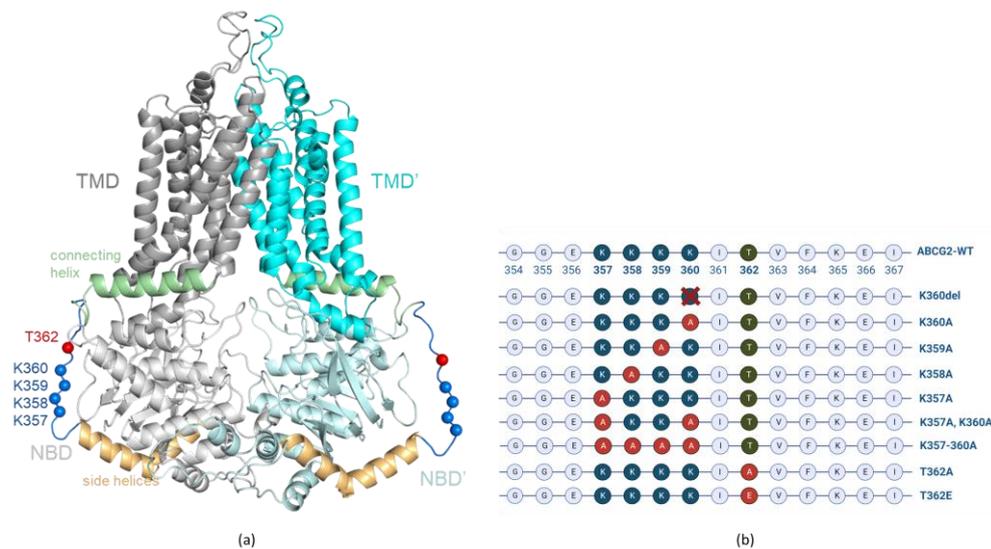

Figure 3. (a) ABCG2 (PDBID: 5hij) structure with modelled loops. Gray, cyan: TMDs; light gray, pale cyan: NBDs; orange: side helices (a.a. 328-353); pale green: connecting helices (a.a. 368-391); blue: disordered loop (a.a. 354-367); blue spheres: Cα of lysine residues from 357 to 360; red spheres: Cα of T362. (b) Schematic representation of the localization of the engineered ABCG2 variants in the unstructured loop (aa. 354-367) region. Figure from our publication [68].

4.1.1 Expression, membrane localization and function of the K357-K360 and T362 ABCG2 mutant variants

Expression of K357A, K358A, K359A, K360A, K357-358-359-360A, K360del, T362A and the T362E ABCG2 variants was examined in cell lines transiently expressing these proteins. HEK293 and HeLa cells were transfected with the p10-CAG-ABCG2-IRES2-GFP vector coding the examined variants. Expression levels were measured three days after transfection. This IRES-based expression system, the GFP expressed from the same vector as the ABCG2 protein, allowed the evaluation of transfection efficiency based on GFP expression.

As shown in Figure 4(a), in most HeLa cells expressing the flexible loop variants, we found similar cell surface expression levels from these ABCG2 variants. The cell surface expression levels of the ABCG2 variants were estimated by measuring 5D3 monoclonal antibody binding, this antibody selectively interacting with the extracellular portion of the ABCG2 protein, in a conformation-sensitive manner, thus the antibody labeling was performed after inhibition of the protein by KO143 inhibitor [67].
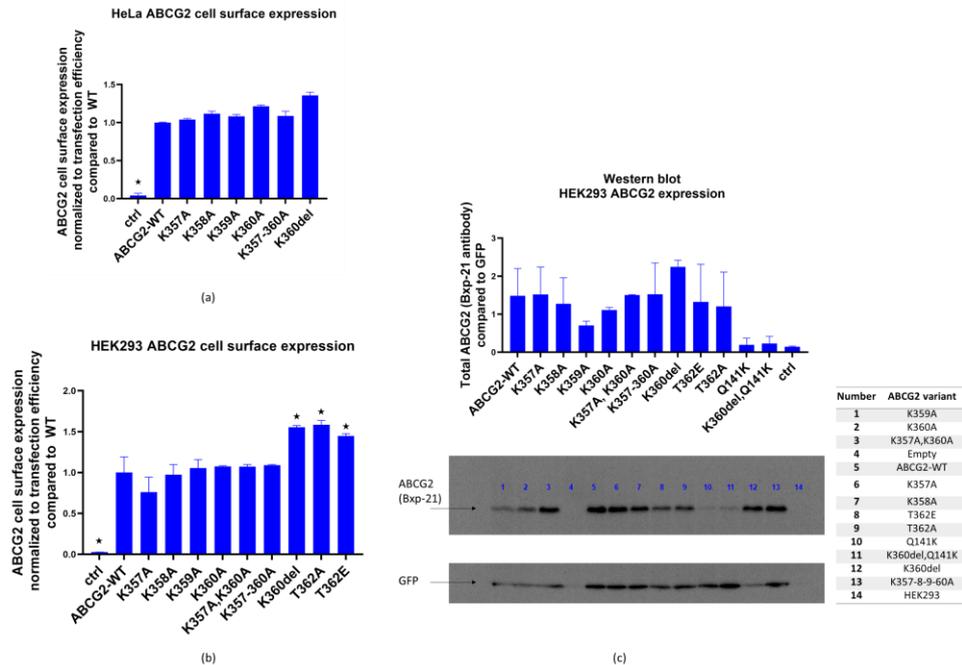

Figure 4. (a). ABCG2 cell surface expression (5D3 binding measured by flow cytometry, normalized to GFP fluorescence for transfection efficiency) in HeLa cells 48 h after transfection with plasmids coding the examined ABCG2 variants (WT, K357A, K358A,

As shown in Figure 4(a,b), all the ABCG2 variants studied reached the cell surface. The ABCG2 expression was normalized to GFP expression, correcting for potential differences in transfection efficiency and other factors affecting vector-based protein expression.

In order to study overall cellular expression levels, Western blot measurements were performed 48 h after the transfection of HEK293 cells, where ABCG2 and GFP proteins were detected in total protein samples from the transfected cells (Figure 4(c)). ABCG2 expression levels were corrected by GFP expression levels. We found variable total expression levels for the variants, with reduced expressions in the cases of K359A and K360A, and an increased level in K360del (these changes, due to the large scattering of the data, were not statistically significant).

To explore whether the K360del variant might rescue the Q141K-ABCG2 variant, which was shown in several studies to have a lower cellular expression[71,72], we have also included the Q141K-ABCG2 and the Q141K-K360del double variant in the Western blot measurements generated in this work. As shown in Figure 4(c), these variants showed relatively low levels of total cellular expression and the expression level of the double mutant was similar to that of the Q141K mutant. As a consequence, lower cell surface expression levels were seen for both the Q141K and Q141K-K360del mutants (see Figure 4 c). Thus, the K360del mutation did not correct the ABCG2-Q141K expression level.

In the following experiments, we measured the transport capacity of the ABCG2 protein in the HEK293 cells transfected by the flexible loop variants. We found that all the ABCG2 variants produced an efficient reduction in the Hoechst33344 dye uptake,

representing the dye extrusion activity of the transporter. This transport activity in all cases was eliminated by the specific ABCG2 transporter inhibitor Ko143. When the multidrug activity factor (MAF) values were calculated from these experiments, these specific activities were similar in the case of all loop variants studied (Figure 5(a) left panel). When comparing transport activity to cell membrane expression levels (5D3 antibody, flow cytometry results, Figure 5(a) right panel), a slight decrease in transport function was observed in the case of the K357A variant.
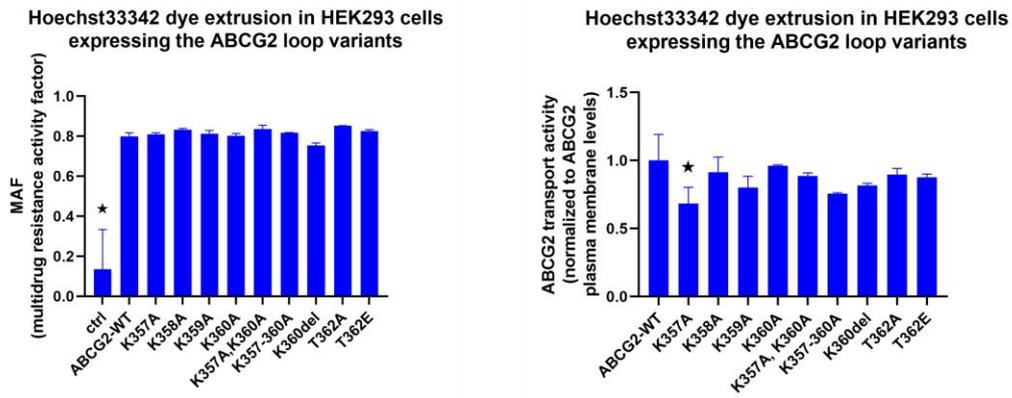
(a)
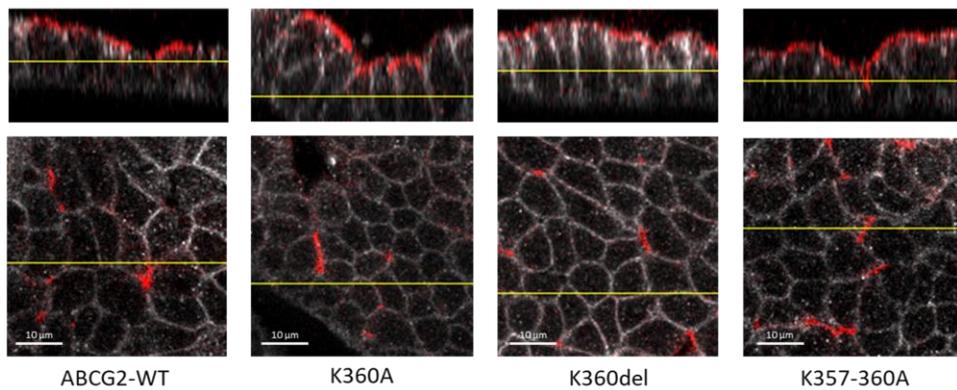
(b)

Figure 5. (a). Hoechst33342 dye extrusion in HEK293 cells expressing the ABCG2 loop variants. Left Panel: MAF (multidrug resistance activity factor) calculated from flow cytometry measurements of dye uptake with or without the Ko143 inhibitor. Right Panel: transport activity normalized for cell surface expression levels of the ABCG2 variants by 5D3 monoclonal antibody binding levels. (b) Confocal images of polarized MDCKII cells expressing ABCG2-WT, K360A, K360del or K357-8-9-60-A variants; red: ABCG2 (Bxp-21 primary antibody, ab3380), white: basolateral Na,K-ATPase (Na,K-ATPase

Data in the literature indicate that the clusters of three or four lysines in unstructured regions of proteins may have significant effects on the cellular distribution, and especially the selective localization of the membrane proteins in polarized cells [73,74]. Since ABCG2 is an apically localized protein in polarized cells [75], in the following experiments it was examined whether deletion or replacement of the lysines in the flexible loop of this protein alters its polarized localization. Therefore, the wild-type and the K360del, K360A and K357-360A ABCG2 variants were expressed in MDCKII cells. To perform localization experiments in polarized cells, MDCKII cells were transfected via the p10-CAG-ABCG2-IRES2-GFP coding transposon-based vectors together with the SB100 Sleeping Beauty transposase. This way a cell population was generated that contained the transposon sequence integrated in the genome. These stable cells expressed ABCG2 even weeks after transfection, thus enabling us to examine ABCG2 after cell polarization.

As shown in Figure 5(b), all these variants were found to be localized in the apical membrane compartments in these polarized cells. Thus, this lysine cluster in the ABCG2 protein does not alter the proper polarized location of this protein.

As a summary, these results indicate that all the variants studied here can reach the cell surface and are fully active transporters. While this was expected by earlier results for the K360del variant [76], the total replacement of the lysine cluster by alanines still showed proper membrane expression, transport activity and apical membrane localization of ABCG2. The data obtained in these experiments also clearly showed that the removal of the T362 phosphorylation site by replacing it with alanine or glutamic acid did not significantly alter the expression, cell surface appearance or the transport function of this protein.

4.1.2 Exploring the effect of inhibition of protein synthesis and proteasomal degradation on the expression of the ABCG2 loop mutant variants K360del and T362A

To monitor the internalization of the ABCG2 constructs, in the following experiments we have inhibited cellular protein synthesis by adding cycloheximide (CHX) to the cell

culturing media of HEK293 cells, expressing the flexible loop mutant variants. As shown in Figure 6, 48 h after transfection, 1–4 h of CHX treatment did not significantly influence the cell surface expression of any of the ABCG2 variants. It has been shown earlier that wild-type ABCG2 has a long (>60 h) plasma membrane half-life [77]; thus, CHX treatment was not expected to decrease the membrane expression levels, while after a longer period this treatment caused significant cell damage and death. Interestingly, internalization of neither the K360del nor the T362A variant was significantly accelerated.
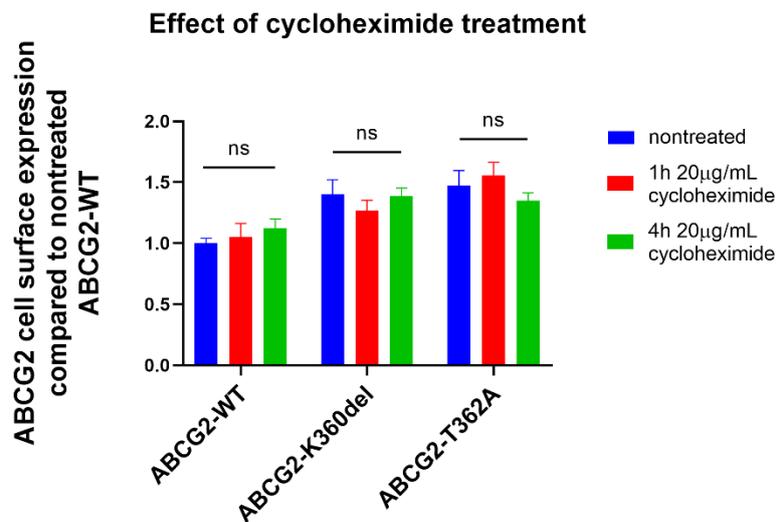

Figure 6. Effect of cycloheximide treatment (1 or 4 h, 20 µg/mL CHX) on ABCG2 cell surface presence (5D3 antibody labeling, measured by flow cytometry) in HEK293 cells transfected with ABCG2-WT, K360del and T362A coding plasmids. CHX treatment was performed 48 h after transfection. For Statistical Analysis, Student's t-test was used. Differences were considered significant when p < 0.05, ns: non-significant. Figure from our publication [68].

4.1.3 Application of the RUSH system to study the cellular trafficking of the K360del and K360A ABCG2 mutant variants

The trafficking of ABCG2 from the ER to the plasma membrane was examined by a specific and efficient experimental method, the dynamic RUSH (Retention Using Selective Hooks) system [78], to the ABCG2 variants [63]. In this method, the protein of interest is tagged with streptavidin-binding peptide (SBP) and GFP, whereas the ER-resident hook protein is tagged with streptavidin. When they are co-expressed, the protein of interest is retained in the ER, from where it can be released by the addition of biotin,

and its trafficking can be tracked from the donor compartment to the target compartment. In this work, a GFP-SBP-ABCG2 fusion protein was co-expressed with an ER hook in HeLa cells. As documented in earlier studies, the N-terminally eGFP-fused ABCG2 was fully active and properly processed in mammalian cells[63,79].

The three variants of ABCG2 examined here were the WT, K360del and the K360A proteins. The synchronized release from the ER initiated by biotin addition allowed us to monitor the cellular trafficking of the ABCG2 variants. To assess the kinetics of their cell surface appearance, an *in situ* immunostaining with a directly labeled 5D3 antibody was performed in non-permeabilized cells, and the colocalization of 5D3 labeling and the GFP fluorescence was determined. The time courses were fitted with a sigmoidal function and the kinetic parameters, including the initial values (CC_0), the limits of the function (CC_{inf}) and the time constants (k), were determined [63].

As shown in Figure 7, the appearance of the K360del variant in the plasma membrane was significantly faster than that of the wild-type ABCG2 (measurements at 2 h), while after 4 h there was no significant difference in the final levels of the variants in the plasma membrane. These data indicate faster cellular trafficking from the ER-released K360del ABCG2 variant compared to the wild-type protein.
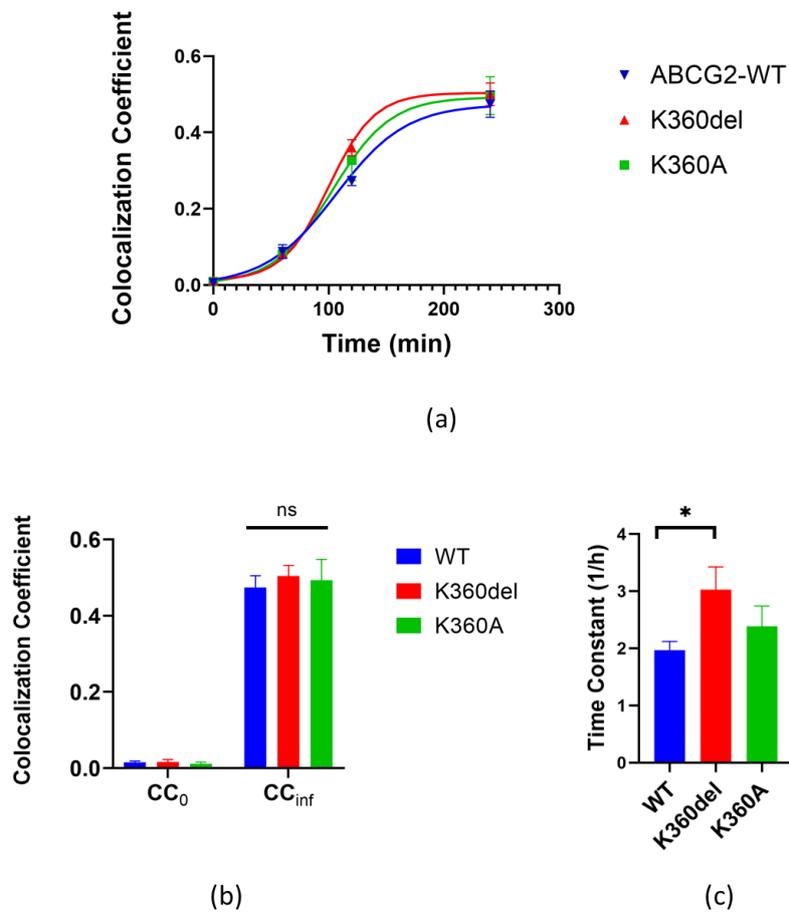
Figure 7. Kinetics of cell surface delivery of WT, K360del and K360A ABCG2 variants. (a) Colocalization coefficients of 5D3 antibody labeling and GFP fluorescence were determined using confocal microscopy images acquired at various time points. The kinetic curves were fitted with sigmoidal function. (b,c) Kinetic parameters of cell surface delivery were derived from the fitted kinetic curves: the initial values (CC0) and the limits of function (CCinf), as well as the time constants (1/h). Data from three independent experiments for all variants. For statistical analyses, Student's t test was used. Differences were considered significant when p < 0.05, marked with a star, ns: non-significant. Figure from our publication [68].

4.2 Examination of the effect of variants on the promoter properties of a regulatory region in the *ATP2B4* gene

The malaria-associated haplotype in the *ATP2B4* gene affects a region up-and downstream the 2nd exon, which was divided into four sequences for detailed analysis. Each sequence (WT and haplotype with SNPs) was cloned into a luciferase plasmid to assess promoter activity in the transfected cells. The four examined regions affected by the SNPs were the H1st, PR2, H1.1, and H1.2 sequences. The H1st, or "Bauer enhancer"

region between the 1st and 2nd exon of the *ATP2B4* gene has been identified by Lessard *et al.* [80] to be an erythroid-specific enhancer, the 2nd exon is an alternative promoter (PR2), and the two additional examined sequences were the intronic H.1.1 and the H1.2 regions downstream from the 2nd exon, as illustrated on Figure 8.
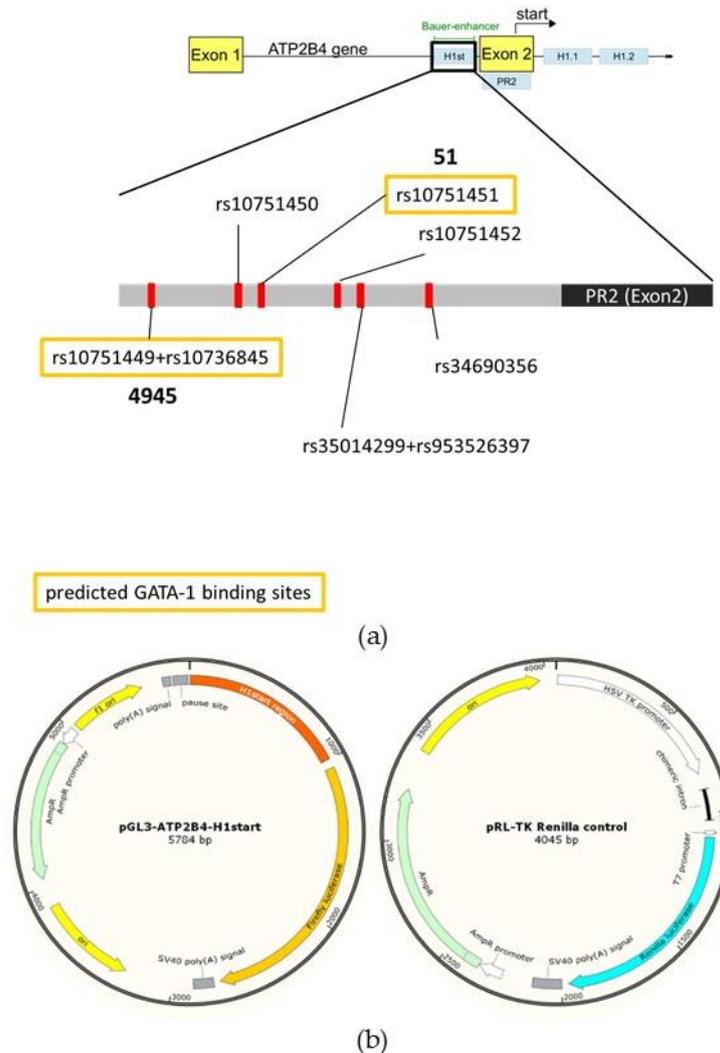
Figure 8. (a) Schematic presentation of the haplotype in the ATP2B4 gene, previously indicated to be responsible for the regulation of PMCA4b expression. In the H1st region, corresponding to the erythroid-specific regulatory region (Bauer-enhancer) described by Lessard et al.[80], the SNPs of the minor haplotype are highlighted. SNPs predicted to eliminate GATA-1 binding sites are labelled by yellow boxes. (b) Plasmids used in the dual luciferase expression assays. Figure from our publication [64].

The WT and haplotype SNP-containing H1st, PR2, H1.1, and H1.2 sequences were tested for promoter activity in the transfected cells. No additional promoter sequences were

included in the Firefly plasmid beyond the tested sequences. HEK293, K562, and HEL cells were transfected with the Firefly vector containing the tested sequence, as well as a vector allowing for Renilla luciferase expression as a control. In the case of the H1.2 region, no promoter activity could be observed (data not shown). For the other three sequences, WT and haplotype sequence Firefly/Renilla luciferase activity ratio in each cell line was calculated, results are shown on Figure 9.
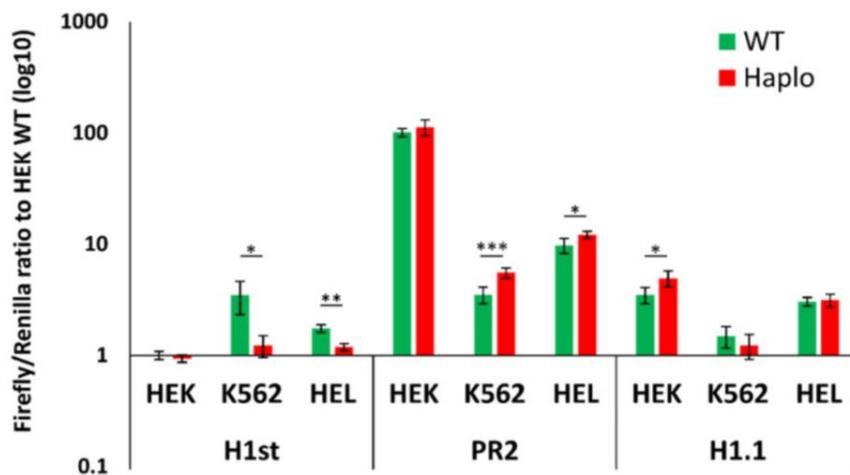

Figure 9. Evaluation of the dual luciferase assay results by comparing the wild-type (WT) and the minor haplotype region (Haplo) driven luciferase expression. The Firefly/Renilla luciferase activity ratio was normalized to the activity obtained in HEK cells with the WT constructs. Mean results and SDs of two biological parallels (each performed with two technical parallels) are shown. (* p<0.05, ** p < 0.01, *** p < 0.001). Figure from our publication [64].

The H1st region showed and increased promoter activity especially in K562 cells compared to HEK cells, and this activity decreased in the case of the haplotype. In the following experiments the H1st region was further investigated by examining the role of the 6 SNPs in the H1-start region of *ATP2B4* (see Figure 8(a)).   Since three SNPs (rs107751449, rs10736845 and rs10751451) in this region affect a predicted GATA-1 transcription factor binding position (Alggen Promo,[81]), a hypothesis was further tested, where the decrease in promoter activity is accounted for an impaired GATA-1 transcription factor binding.

To validate that GATA-1 is indeed only expressed in the examined erythroid cell lineages, GATA-1 mRNA levels were confirmed by reverse transcription PCR (RT-PCR) in the cell lines used for the experiments. As shown in Figure 10(a), HEK cells do not express

measurable amounts of GATA-1 mRNA, while GATA-1 mRNA is present in the K562 and HEL cells. To further validate the lack of GATA-1 protein in HEK cells, Western blot with anti-GATA-1 antibody was performed. No GATA-1 expression could be observed in HEK293 cells, while in K562 and HEL cells the protein was present (Figure 10(b)). This expression pattern highlights that the selected cell lines are suitable models to test the hypothesis that the GATA-1 transcription factor plays a role in the mechanisms underlying the observed differences between the HEK cells and the two erythroid cell lines.

To further examine the role of GATA-1 in the enhancer activity, HEK, K562 and HEL cells were transfected with an expression vector containing the GATA-1 coding cDNA. The dual luciferase assay was performed in these GATA-1-overexpressing cells (Figure 10(c)). In these experiments the luciferase expression constructs contained either the WT or the minor haplotype variant of the H1st sequence. In the case of the HEK cells, GATA-1 overexpression only slightly increased the luciferase expression, both in the case of the WT and minor haplotype constructs. In contrast, GATA-1 overexpression greatly increased luciferase expression in the K652 and HEL erythroid cells. High luciferase expression by GATA-1 co-expression in the erythroid cell lines was significantly more pronounced from the plasmid containing the wild-type H1-start than that containing the minor variant of this region.
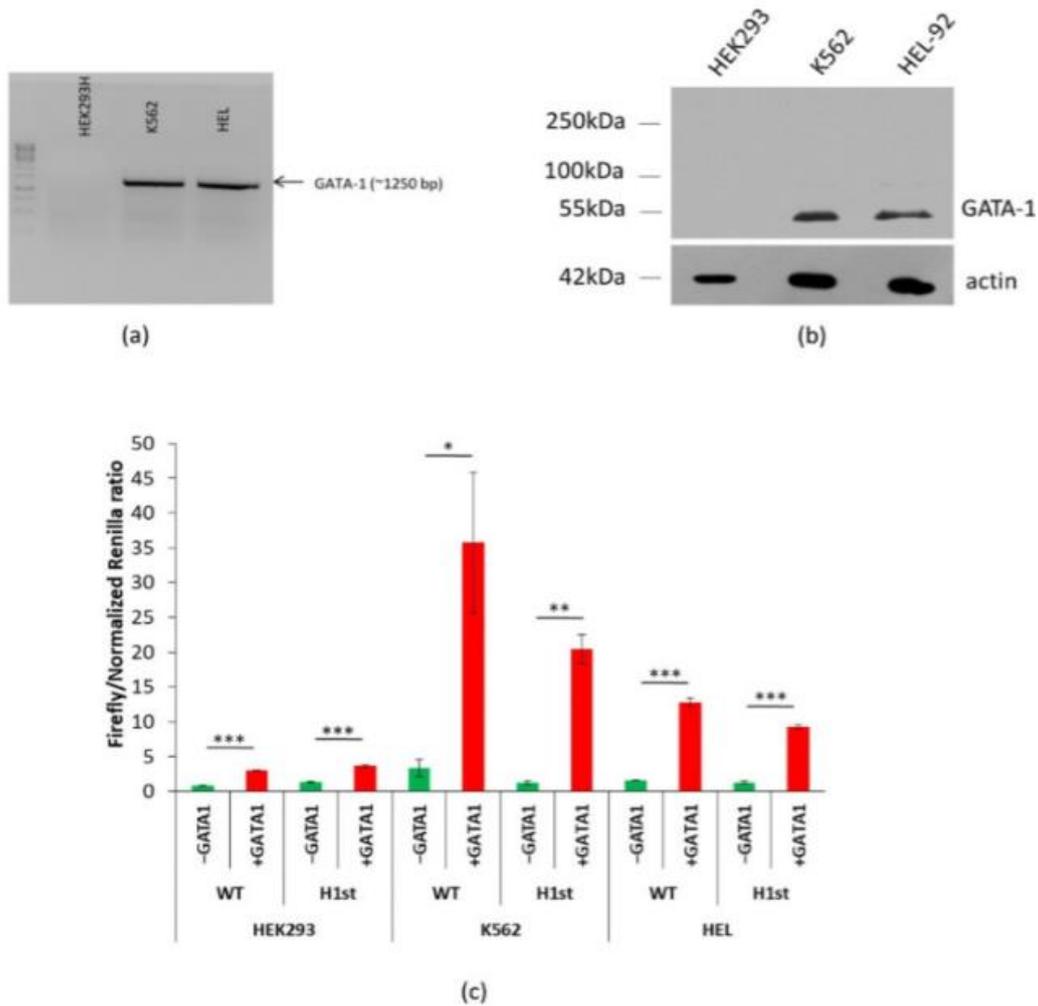
Figure 10. Potential role of GATA-1 in the regulation of PMCA4B expression. For details see the Methods section. (a) GATA-1 mRNA expression in HEK, K562 and HEL cells. (b) GATA-1 protein expression HEK, K562 and HEL cells – Western blot of total protein extractions from HEK293, K562 and HEL-92 cells with anti-GATA-1 and anti-actin primary, HRP-labeled secondary antibodies. (c) Dual luciferase assay in the GATA-1-expressing, transfected cells. The inserted WT or the minor haplotype (H1) versions of the ATP2B4 regions were expressed in HEK, K562 and HEL cells. The ratio of the Firefly/Renilla luciferase activity is shown. The error bars represent the SDs of two biological parallels. Significance by t-test: * p < 0.05, ** p < 0.01, *** p < 0.001. Figure from our publication [64].

In the further experiments we focused on the individual impact of the SNPs in the predicted GATA-1 transcription factor binding sites within the H1-start region. Therefore, the SNP-s (rs107751449, rs10736845 and rs10751451) in the predicted GATA-1 transcription factor binding sites were selectively mutated. Luciferase expression constructs containing the minor variant SNPs, rs107751449+rs10736845 (4945, as in

Figure11), and constructs containing only the SNP rs10751451 ("51" in Figure 11) were generated. A construct containing the three minor variant SNPs predicted to impair GATA-1 binding, rs107751449, rs10736845 and rs10751451 ("4945/51" in Figure 11), was also generated and tested in K562 cells.
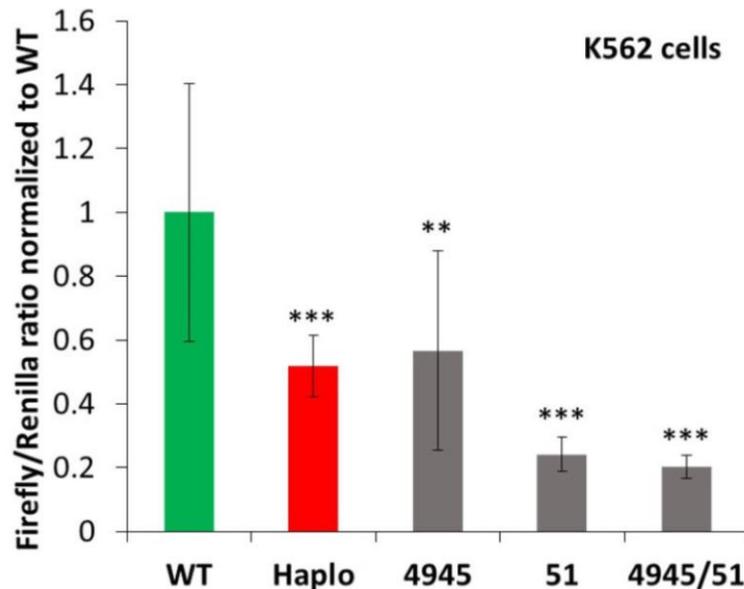
Figure 11. The role of selected SNPs in modulating Firefly luciferase expression in the dual luciferase assay, performed in the K562 erythroid cells. The ratio of the Firefly/Renilla luciferase activity is shown. The error bars represent the SDs of two biological parallels. (** p < 0.01, *** p < 0.001). Figure from our publication [64].

As shown in Figure 11, when expressing these constructs in K562 cells, we found that the expression of the full minor haplotype strongly reduced luciferase expression compared to the WT sequence (see also Figure 9). A similar reduction was observed in the case of the construct containing the two SNPs predicted in one of the GATA-1 binding regions (4945, rs107751449+rs10736845). Interestingly, construct 51 (containing only the minor variant of SNP, rs10751451), also predicted to be involved in GATA-1 binding, caused an even larger reduction in luciferase expression, and the construct containing all three SNPs (4945/51), similarly to 51, greatly reduced luciferase expression.

4.3 Producing the SARS-CoV-2 RBD protein and using it in an ELISA test to measure serum antibody levels of COVID-19 patients and vaccinated healthy individuals

4.3.1 Generating HEK293 cell lines that stably produce the SARS-CoV-2 (Wuhan, Omicron BA.1 and BA.5 variants) spike RBD protein

HEK293 cells stably expressing the Wuhan-RBD protein were generated using the SB100x Sleeping Beauty transposase and the p10 transposon-coding vector, which includes the sequence that was stably integrated into the genome of the cells. The RBD protein was N-terminally tagged by the novel N-terminal signal peptide of the SARS-CoV-2 spike protein and included a C-terminal His-tag. EGFP expression was secured from the same mRNA by the IRES2, sorting for positive cells was performed based on fluorescence. This solution also helped in everyday monitoring of the positive cells via fluorescence microscopy. The examples in Figure 12 and Figure 13 show the Wuhan-RBD vector and the detection of the produced RBD (Wuhan variant) protein. In the case of the Omicron BA.1 and BA.5 RBD variants, the sequences containing mutations of the Omicron BA.1 and the BA.5 were custom made and inserted into the p10 vector. The Omicron RBD proteins produced by the cell lines were not recognized by the monoclonal anti-RBD specific antibodies, they could only be detected via Western blot by the anti-His antibody.
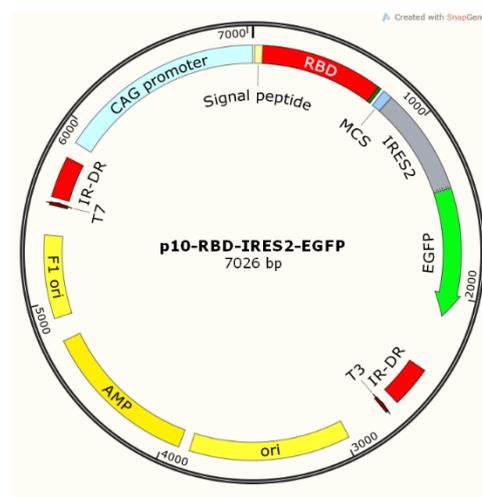
Figure 12: The p10-RBD-IRES2-EGFP transposon vector map. HEK293 cells were generated using this and the SB100x transposase coding vector, to allow stable genome integration of the CAG-RBD-IRES2-EGFP sequence. Figure from the supplementary materials of our publication [82].

Stable cell lines derived from single cells were characterized by their RBD protein production. Western blot and ELISA assays performed by commercial, specific antibodies against the RBD confirmed the production of the RBD by the cell lines.
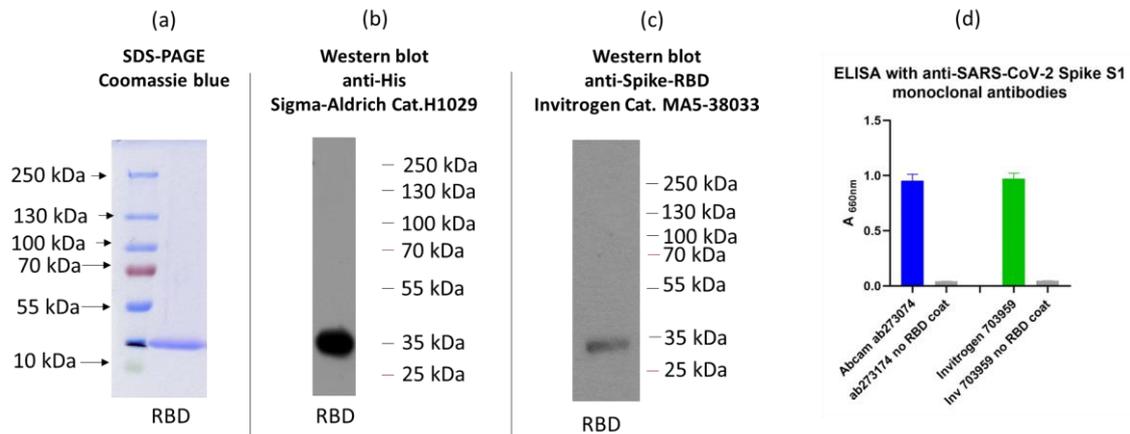
Figure 13. The RBD production was examined by SDS-polyacrylamide gel electrophoreses and Western blotting. (a) Shows the purified RBD protein after SDS-PAGE and Coomassie blue staining. (b) Shows the purified RBD protein after SDS-PAGE and western blot using the anti-His primary antibody (Sigma-Aldrich Cat.H1029). (c) Shows the purified RBD protein after SDS-PAGE and western blot using the anti-RBD primary antibody (Invitrogen Cat. MA5-38033). (d) ELISA results of RBD(Wuhan) detected by two anti-SARS-CoV-2 Spike S1 commercially available monoclonal antibodies (Abcam Cat. ab273074 and Invitrogen Cat. 703959), controls: ELISA coating without RBD. Figure from our publication [82].

4.3.2 Using the SARS-CoV-2 RBD protein (Wuhan and Omicron variants) in a simple ELISA assay
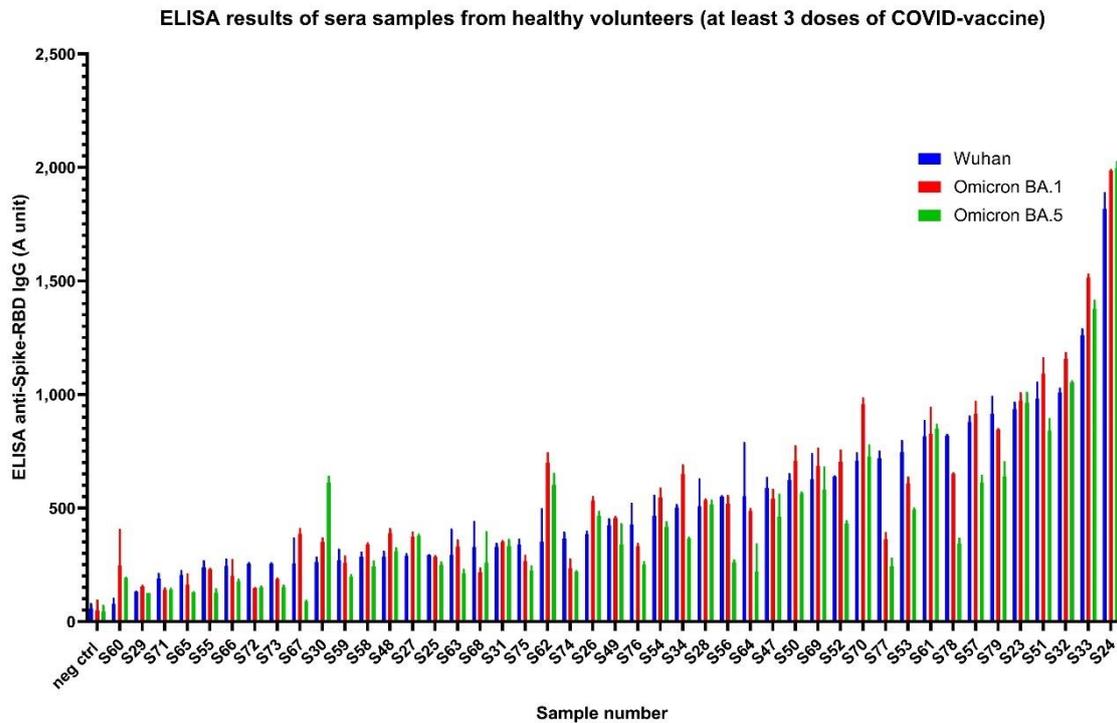
Figure 14. ELISA results of sera samples from healthy, vaccinated individuals (at least 3 doses of COVID-vaccine). Figure from our publication [82].

Sera samples were collected from healthy, fully vaccinated individuals during the 2022-2023 winter period. All individuals in this study received at least three vaccine shots, the monovalent two-dose BNT162b2 (Pfizer-BioNTech, commercial name: Comirnaty) or mRNA-1273 (Moderna-NIAID) (commercial name: Spikevax) vaccines, and at least one booster shot (either homologous or heterologous forms of these vaccines). As shown in Figure 14, huge individual differences could be observed in antibody levels.
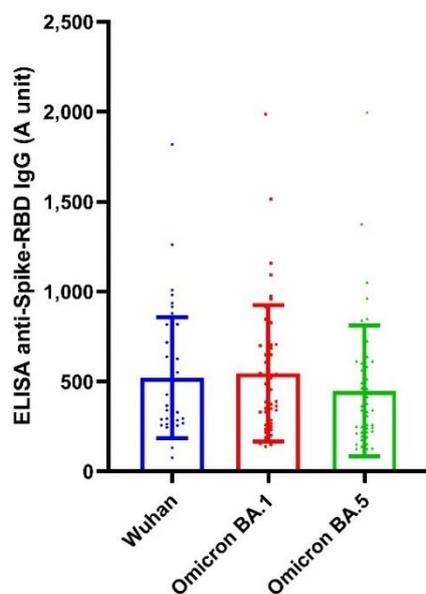
Figure 15. Antibody levels against the Wuhan, the Omicron BA.1 and the Omicron BA.5 SARS-CoV-2 RBD. No difference between antibody levels against the examined variants could be observed. Figure from our publication [82].

When grouping the fully vaccinated individuals' anti-RBD IgG antibody levels to the Wuhan, Omicron BA.1 and BA.5 variants, no significant difference could be observed in antibody levels against the Wuhan and Omicron RBD variants.
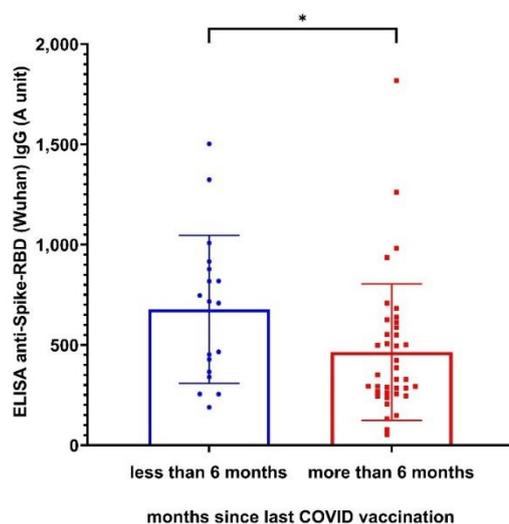
Figure 16. anti-spike RBD IgG antibody levels of healthy, vaccinated individuals, categorized by months since last COVID vaccination. Two-tailed unpaired t-test (95% confidence interval) showed significant difference between the two groups. Figure from our publication [82].

If we examined the results from another aspect, 6 months after the latest vaccination or exposure to the virus, antibody levels decrease. This difference could be observed in the fully vaccinated individuals, when the time after exposure was determined by either the latest vaccination date or, if it was closer, the latest COVID-19 illness date.
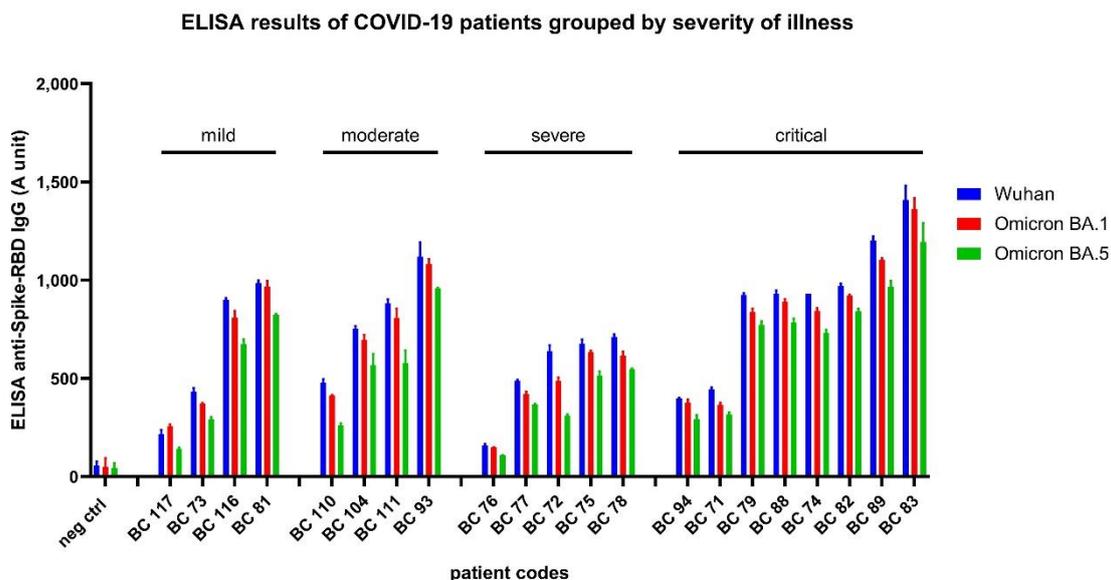
Figure 17. anti-Spike RBD (Wuhan, Omicron BA.1, Omicron BA.5) IgG ELISA results of COVID-19 patients during the second COVID wave of the pandemic, unvaccinated patients, grouped by COVID illness severity (mild, moderate, severe, critical). Figure from our publication [82].

COVID-19 patients examined and/or treated in the National Korányi Institute of Pulmonology in Hungary, in the period of January 2020 – November 2021, with various manifestations of the COVID-19 disease. Patients were grouped by severity, mild cases: patient recovered at home, without hospital treatment; moderate: patient recovered after hospital treatment, but not at the intensive care unit; severe: patient recovered from illness after hospital treatment at the intensive care unit; critical: patient recovered from illness after hospital treatment at the intensive care unit, with mechanical ventilation.

The collected sera after convalescence (within 7 days after recovery from illness) were stored at -80 C. During the time these samples were collected, the Omicron virus variants were not present in Hungary.
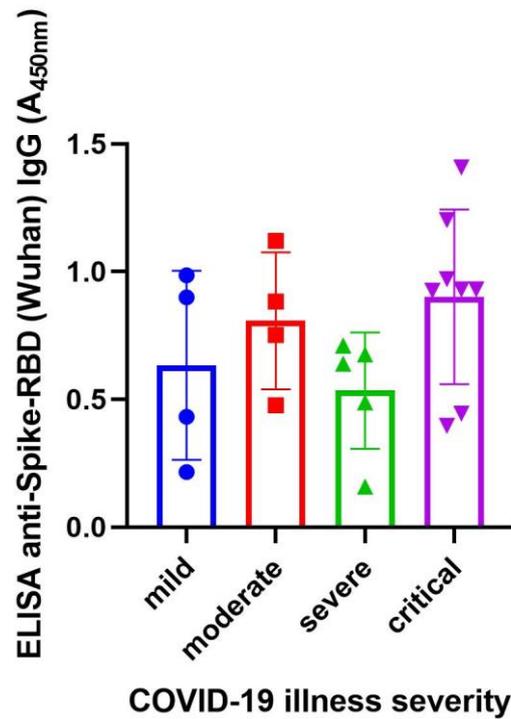
Figure 18. Average anti-Spike RBD IgG ELISA results (Wuhan, Omicron BA.1, Omicron BA.5) of COVID-19 patients during the second COVID wave of the pandemic, unvaccinated patients. Averages calculated in COVID-19 disease severity groups. Figure from our publication [82].

These results indicate a cross-reactivity of the antibodies generated in the convalescent patients against the examined Omicron variants. Although no significant difference in the average variant-specific antibody levels could be observed (Figure 15), a tendency on an individual level points to slightly decreased antibody recognition in the case of the Omicron BA.5 variant, the ratio of IgG levels observed against the Omicron BA.5/Wuhan variant was 0.87.

Huge individual differences could be observed in antibody levels against the SARS-CoV-2 Spike RBD in COVID-19 patients. Although there is a tendency for higher anti-RBD IgG levels in patients with COVID-19 disease at a critical level, the number of patients examined here is not enough to provide a quantitation of this potential difference. (Figure 18)

5 Discussion

In this work, a naturally occurring missense variant in the ABCG2 membrane protein was examined in HEK293, HeLa and MDCK cell lines by examining and alanine mutants of ABCG2 in the affected region. Another project involving naturally occurring variants of a membrane protein focused on SNPs in a haplotype of the PMCA4b calcium transporter coding *ATP2B4* gene regulatory region were characterized by their erythroid-specific effect on promoter activity. The SARS-CoV-2 spike RBD antigen was produced in HEK293 cell line, utilizing some of the methods used in the previous work to overexpress membrane proteins. The RBD protein product was used in a simple ELISA assay to determine serum antibody levels against the Wuhan and Omicron variants of the SARS-CoV-2 spike RBD.

When examining the intracellular loop in the ABCG2 protein [83], examining the alanine variants of the four consecutive lysines in the disordered loop, none of the alanine variants showed the same effect as observed in the case of the K360del variant. The K360del variant showed an elevated surface expression level in HEK293 cells, and this elevated trend was observed in HeLa cells and total protein expression analysis via Western blot, although not significant. The K360del showed normal apical localization in polarized MDCK cells, based on this, it can be supposed that the four lysines are not involved in polarization. Several hypotheses were tested in the experiments, to uncover the molecular mechanism this disordered loop is involved in. Finally, the RUSH system helped to investigate the trafficking of the K360del variant from the endoplasmic reticulum to the plasma membrane, which revealed that this variant has faster trafficking, reaching the plasma membrane faster compared to the WT. This result should help us better understand this disordered loop, which might play a role in trafficking. There are variants of the ABCG2 transporter known to have decreased trafficking, including the most common variant, the Q141K[63].

The PIM kinase-dependent T362 phosphorylation was suggested to be crucially important for both the membrane insertion and function of the ABCG2 transporter [69,70]. It has also been suggested that the inhibition of this kinase and the connected PI3K/Akt signaling pathway, activated in many human tumors, might be an important drug target for reducing ABCG2-related cancer drug resistance. According to the results of our research, the T362A variant, where this phosphorylation site is altered, the protein is

expressed normally, similar to the wild type ABCG2, and functions well. This finding contradicts a previous finding in the literature. Whether the different methods used in the two independent experiments could be the cause of this difference, is still to be resolved. Our experiments involved an untagged ABCG2, while in the previous literature, an N-terminal HA-tagged form of the protein was used. Our experiments, where only the 362 threonine was replaced, questioned the regulatory role of this residue.

The outcomes of this research contribute to potential applications in therapeutic treatment and development. The findings on ABCG2 trafficking and the T362 residue phosphorylation-independent regulation may influence future drug design. From a clinical and pharmacological perspective, carriers of the K360del variant should be considered as patients with a normally functioning ABCG2.

According to our results [64]**, the potential regulatory H1start region in the _ATP2B4_ gene indeed had significant promoter/enhancer activity in all cell lines examined.** This activity was not altered by the presence of the minor variant SNPs in the non-erythroid HEK cells, while in the erythroid cell lines, the minor variant of the H1-start region had a significantly reduced promoter/enhancer activity as compared to the wild-type sequence. In addition, the overexpression of GATA-1 increased the promoter/enhancer activity of the examined regions in HEK293 cells independent of the presence or absence of SNPs, while this effect of GATA-1 was significantly more pronounced in the erythroid cell lines, and strongly reduced in the presence of the minor variant of the H1-start region.

To further explore the role of specific sequences, the SNPs predicted to be involved in GATA-1 binding within the H1-start region were selective examined, and expressed the luciferase-based reporter construct in the erythroid K562 cell line. These experiments indicated that the two predicted GATA-1 binding sites, eliminated by the presence of minor SNPs, are both functionally important in the erythroid cells. The luciferase expression constructs containing these affected minor SNPs, that is rs107751449+rs10736845, or rs10751451, had significantly reduced promoter/enhancer activity. Interestingly, the minor variant of rs10751451 had a more pronounced effect on this activity, either used separately, or together with the other two SNPs. The results, which indicate a greater decrease in H1st promoter activity for the rs10751451 SNP alone compared to all SNPs of the minor haplotype combined, underline the complexity of this

regulatory mechanism. Interestingly, a [84] similar role of a polymorphic GATA-1 binding site in the promoter region has been documented in modulating the expression of the Duffy blood group antigen, a receptor for Plasmodium in the erythroid cells, thus reducing malaria infection [84,85].

In recent literature, the connection between PMCA4b and malaria has received increasing attention. A current study in mice with systemic knock-out of PMCA4 indicated that in these KO mice, malaria infection has a more pronounced central nervous system effect [86].

While our results document the functional role of a haplotype region (H1st) and SNPs in GATA-1 regulation of *ATP2B4* expression in erythroid cells, these results also suggest that in addition to GATA-1, other uncovered factors may also be involved in the erythroid-specific regulation of this region. This is supported by our GATA-1 co-expression studies (Figure 10c), where the overexpression of GATA-1 in HEK cells did not result in the same elevation of promoter activity as in K562 and HEL cells, suggesting that apart from GATA-1, other erythroid-specific mechanisms are playing a role in this regulation.

By identifying and characterizing the effect of specific SNPs that impact *ATP2B4*, we are getting closer to understanding the detailed molecular-level regulation of a key membrane protein, PMCA4b. These insights not only aid our understanding of the regulatory mechanisms underlying PMCA4b expression but also highlight how inherited genetic variability can influence cellular calcium handling and susceptibility to diseases like malaria. Understanding these SNP-related effects could guide therapeutic strategies aimed at modulating PMCA4b activity, particularly in disease contexts where altered calcium homeostasis plays a role.

Immune response against the SARS-CoV-2 virus has become a widely studied question during the COVID-19 pandemic. It has been reported early on that the most important antigen of SARS-CoV is the spike protein, and more specifically, the receptor binding domain of the spike protein [87,88]. The RBD connects to the ACE2 receptor when the virus enters the infected cells. Most of the neutralizing antibodies recognize the RBD, and the world-wide used vaccines resulted in antibody protection against the spike protein. Most of the antibody tests measure antibody levels against the spike, sometimes the Nucleocapsid protein, which is more conserved among coronaviruses [89]. Emerging

new variants that cause concern ever since the beginning of the pandemic, often include mutations in the RBD of the spike protein. Some of these mutations mean altered recognition by neutralizing antibodies, thus resulting in some level of escape in immunized individuals. The spike protein, and the RBD (including its variants) became an important protein product for the diagnostic industry.

In this work, my goal was to produce the spike-RBD (Wuhan and Omicron variants) in mammalian cell lines and use them in an ELISA assay to measure variant-specific antibody levels. The stable production of these proteins was achieved by stably introducing the RBD-coding sequence into the genome of the HEK293 cells and securing the extracellular secretion. This was ensured by the novel N-terminal signal of the Spike protein, which allowed for extracellular secretion of the RBD into the cell culture media (amino acids from the spike protein 1–14; MFVF…VSSQ), along with a C-terminal hexahistidine tag to allow for downstream processing and separation of the protein. This RBD sequence modification was developed by Amanat et al [61], which was transferred to the Sleeping Beauty expression system.

The Omicron variant-specific sequences of the RBD were custom-ordered and inserted into the same vector system used for the Wuhan-type RBD production. HEK293 cells stably expressing the RBD were adapted to serum-free growth. Cells were characterized and the clones showing the best yields were selected.

IgG antibody levels against the Wuhan and different Omicron variants from serum samples were determined by a simple ELISA assay. Although due to high individual variations, no significant difference could be observed in the average antibody levels against the examined Omicron and the original Wuhan variant, a tendency of slightly decreased antibody levels against the Omicron BA.5 on the individual level can be seen in both healthy vaccinated individuals and COVID-19 patients. Significant difference could be observed in the antibody levels according to the time since the last vaccination, which supports data in the literature [53]. Antibody levels fade over time, and it has to be noted that protective long-term immunity might not be best determined solely based on antibody levels.

The HEK293 cell lines were shown to be suitable for serum-free, suspension culture protein production, and the produced protein preserved the biological antigenic properties after downstream processing. Apart from the application [82] presented here, this protein

product was used in a study to determine interaction between SARS-CoV-2 and a PARP inhibitor [90]. Together with our collaborators, the downstream processing of the cell culture media was optimized, which makes this cell line suitable for large-scale protein production. [91]

The ELISA assay shown here is an example of how rapid production and application of viral antigens can support monitoring of immune protection across variants.

These findings should contribute to our understanding of membrane protein variants in both basic biological research and clinical applications. They provide insights that could contribute to personalized drug treatments, enhance malaria therapies, and improve responses to viral outbreaks.

6　Conclusions

- The ABCG2 transporter contains a disordered cytoplasmic loop, one of the four consecutive lysines in the loop is deleted in the K360del variant because of a naturally occurring SNP (rs750972998). Based on the results presented here, when one of the four lysines is missing, the trafficking from the endoplasmic reticulum to the plasma membrane is a little faster than in the case of the WT-ABCG2. No big difference in the expression, function and localization of the studied loop variants could be shown. When expressing the ABCG2-T362 mutant T362A, no decrease in protein expression or function could be observed compared to the WT-ABCG2. This result is contradictory to a previous report in the literature, where this site was proposed to be a crucial phosphorylation in the ABCG2 protein.

- The PMCA4b calcium transporter has been reported to be regulated by a haplotype affecting an alternative promoter region of the *ATP2B4* gene. This minor haplotype has been shown in GWAS to decrease the risk of severe malaria. Detailed examination of the SNPs in the haplotype was carried out in the presented work. The results identify one of four shorter regions of the *ATP2B4* gene affected by the haplotype, and the specific SNPs within this shorter region (H1st) that affected a predicted GATA-1 erythroid-specific transcription factor binding site. These single SNPs of the minor variant lead to decreased promoter activity in erythroid K562 cells, which could be the reason for decreased PMCA4b protein expression in the RBCs of carriers of this haplotype. These results give more insight into the molecular-level, erythroid-specific regulation of PMCA4b expression through SNPs in the malaria-associated *ATP2B4* haplotype.

- This work included the production of the Wuhan, Omicron BA.1 and Omicron BA.5 SARS-CoV-2 Spike RBD protein by stably expressing HEK293 cell lines. A simple diagnostic application in an ELISA test to determine variant-specific anti-RBD antibody levels from healthy, vaccinated individuals and COVID-19 patients of four severity groups was performed. Huge individual differences could be observed among healthy vaccinated individuals and COVID-19 patients treated in the hospital. No significant difference could be observed between the different severity groups, although several hospitalized patients showed extremely elevated antibody levels. The results show how antibody levels decrease 6 months after immunization (vaccination or infection).

7 Summary

The presented results contribute to our understanding of naturally occurring variants of three clinically important membrane proteins, the multidrug transporter ABCG2 and the PMCA4b calcium pump, and the SARS-CoV-2 spike protein.

Missense ABCG2 variants often lead to decreased function of the protein, but the K360del variant examined here seems to be expressed in normal amounts and functional. The trafficking of the variant from the endoplasmic reticulum to the plasma membrane was faster in the experiments, which poses interesting questions about the role of this disordered intracellular loop of this protein. Surprisingly, the T362A ABCG2 variant was normally expressed and functional, contradictory to a previous report in the literature. Based on the results shown here, unlike many of the variants resulting in amino acid change in ABCG2, the K360del variant should be considered as a variant with normal function.

A haplotype in the PMCA4b coding *ATP2B4* gene has been linked to less severe malaria and decreased red blood cell PMCA4b expression levels. This study showed detailed examination of the effect of SNPs within the *ATP2B4* gene on promoter activity in erythroid cell lines (HEK and K562) and in control HEK cells using the dual luciferase assay. When testing individual effects of the SNPs within the haplotype in the H1st region on promoter activity in K562 cells, 3 SNPs that could be responsible for the decreased expression levels were identified. These results together support the hypothesis that GATA-1 transcription factor binding is impaired if specific SNPs of the minor haplotype are present.

This work also included the generation of stable, suspension HEK cell lines that produce the SARS-CoV-2 spike RBD protein and their application in an ELISA assay. Serum IgG antibody levels of healthy, vaccinated individuals and hospitalized COVID-19 patients against the Wuhan and Omicron variants were measured. Results show how antibody levels fade over time, with significant decrease 6 months after vaccination or infection.

Although the scientific questions explored in the presented research projects were diverse, they all utilized expression and overexpression systems in human cell lines. These tools have proven to be effective for studying membrane protein variants from multiple perspectives. The findings presented in this dissertation aim to highlight the critical role of variant-specific studies in addressing complex biological and clinical challenges.

8   References

[1]   L. Guan, The rapid developments of membrane protein structure biology over the last two decades, BMC Biol 21 (2023) 300. https://doi.org/10.1186/s12915-023-01795-9.

[2]   L.A. Doyle, W. Yang, L. V Abruzzo, T. Krogmann, Y. Gao, A.K. Rishi, D.D. Ross, A multidrug resistance transporter from human MCF-7 breast cancer cells., Proc Natl Acad Sci U S A 95 (1998) 15665–70. https://doi.org/10.1073/pnas.95.26.15665.

[3]   G.L. Scheffer, M. Maliepaard, A.C.L.M. Pijnenborg, M.A. van Gastelen, M.C. de Jong, A.B. Schroeijers, D.M. van der Kolk, J.D. Allen, D.D. Ross, P. van der Valk, W.S. Dalton, J.H.M. Schellens, R.J. Scheper, Breast Cancer Resistance Protein Is Localized at the Plasma Membrane in Mitoxantrone- and Topotecan-resistant Cell Lines1, Cancer Res 60 (2000) 2589–2593.

[4]   R. Allikmets, L.M. Schriml, A. Hutchinson, V. Romano-Spica, M. Dean, A human placenta-specific ATP-binding cassette gene (ABCP) on chromosome 4q22 that is involved in multidrug resistance., Cancer Res 58 (1998) 5337–9.

[5]   M. Maliepaard, G.L. Scheffer, I.F. Faneyte, M.A. van Gastelen, A.C. Pijnenborg, A.H. Schinkel, M.J. van De Vijver, R.J. Scheper, J.H. Schellens, Subcellular localization and distribution of the breast cancer resistance protein transporter in normal human tissues., Cancer Res 61 (2001) 3458–64.

[6]   M.L.H. Vlaming, J.S. Lagas, A.H. Schinkel, Physiological and pharmacological roles of ABCG2 (BCRP): Recent findings in Abcg2 knockout mice, Adv Drug Deliv Rev 61 (2009) 14–25. https://doi.org/10.1016/j.addr.2008.08.007.

[7]   S. Zhou, J.D. Schuetz, K.D. Bunting, A.-M. Colapietro, J. Sampath, J.J. Morris, I. Lagutina, G.C. Grosveld, M. Osawa, H. Nakauchi, B.P. Sorrentino, The ABC transporter Bcrp1/ABCG2 is expressed in a wide variety of stem cells and is a molecular determinant of the side-population phenotype, Nat Med 7 (2001) 1028–1034. https://doi.org/10.1038/nm0901-1028.

[8]   J.-T. Zhang, Biochemistry and pharmacology of the human multidrug resistance gene product, ABCG2., Zhong Nan Da Xue Xue Bao Yi Xue Ban 32 (2007) 531–41.

[9]   X. Ding, J. Wu, C. Jiang, ABCG2: A potential marker of stem cells and novel target in stem cell and cancer therapy, Life Sci 86 (2010) 631–637. https://doi.org/10.1016/j.lfs.2010.02.012.

[10]   European Medicines Agency, Committee for Medicinal Products for Human Use (CHMP), ICH Guideline M12 on Drug Interaction Studies: Step 2b, 2022. https://www.ema.europa.eu/en/documents/scientific-guideline/draft-ich-guideline-m12-drug-interaction-studies-step-2b_en.pdf (accessed October 7, 2024).

[11]   U.S. Food and Drug Administration, Clinical Drug Interaction Studies — Cytochrome P450 Enzyme- and Transporter-Mediated Drug Interactions, 2020. https://www.regulations.gov/document/FDA-2017-D-5961-0023 (accessed October 8, 2024).

[12]   K.L. Fung, M.M. Gottesman, A synonymous polymorphism in a common MDR1 (ABCB1) haplotype shapes protein function., Biochim Biophys Acta 1794 (2009) 860–71. https://doi.org/10.1016/j.bbapap.2009.02.014.

[13]   K.M. Hoque, E.E. Dixon, R.M. Lewis, J. Allan, G.D. Gamble, A.J. Phipps-Green, V.L. Halperin Kuhns, A.M. Horne, L.K. Stamp, T.R. Merriman, N. Dalbeth, O.M. Woodward, The ABCG2 Q141K hyperuricemia and gout associated variant illuminates the physiology of human urate excretion, Nat Commun 11 (2020) 2767. https://doi.org/10.1038/s41467-020-16525-w.

[14]   A. Dehghan, A. Köttgen, Q. Yang, S.J. Hwang, W.L. Kao, F. Rivadeneira, E. Boerwinkle, D. Levy, A. Hofman, B.C. Astor, E.J. Benjamin, C.M. van Duijn, J.C. Witteman, J. Coresh, C.S. Fox, Association of three genetic loci with uric acid concentration and risk of gout: a genome-wide association study, The Lancet 372 (2008) 1953–1961. https://doi.org/10.1016/S0140-6736(08)61343-4.

[15]   H. Matsuo, T. Takada, K. Ichida, T. Nakamura, A. Nakayama, Y. Ikebuchi, K. Ito, Y. Kusanagi, T. Chiba, S. Tadokoro, Y. Takada, Y. Oikawa, H. Inoue, K. Suzuki, R. Okada, J. Nishiyama, H. Domoto, S. Watanabe, M. Fujita, Y. Morimoto, M. Naito, K. Nishio, A. Hishida, K. Wakai, Y. Asai, K. Niwa, K. Kamakura, S. Nonoyama, Y. Sakurai, T. Hosoya, Y. Kanai, H. Suzuki, N. Hamajima, N. Shinomiya, Common defects of ABCG2, a high-capacity urate exporter, cause gout: A function-based

genetic analysis in a Japanese population, Sci Transl Med 1 (2009). https://doi.org/10.1126/scitranslmed.3000237.

[16] T. Higashino, T. Takada, H. Nakaoka, Y. Toyoda, B. Stiburkova, H. Miyata, Y. Ikebuchi, H. Nakashima, S. Shimizu, M. Kawaguchi, M. Sakiyama, A. Nakayama, A. Akashi, Y. Tanahashi, Y. Kawamura, T. Nakamura, K. Wakai, R. Okada, K. Yamamoto, K. Hosomichi, T. Hosoya, K. Ichida, H. Ooyama, H. Suzuki, I. Inoue, T.R. Merriman, N. Shinomiya, H. Matsuo, Multiple common and rare variants of ABCG2 cause gout, Rheumatic & Musculoskeletal Diseases 3 (2017). https://doi.org/10.1136/rmdopen-2017-000464.

[17] H. Matsuo, K. Ichida, T. Takada, A. Nakayama, H. Nakashima, T. Nakamura, Y. Kawamura, Y. Takada, K. Yamamoto, H. Inoue, Y. Oikawa, M. Naito, A. Hishida, K. Wakai, C. Okada, S. Shimizu, M. Sakiyama, T. Chiba, H. Ogata, K. Niwa, M. Hosoyamada, A. Mori, N. Hamajima, H. Suzuki, Y. Kanai, Y. Sakurai, T. Hosoya, T. Shimizu, N. Shinomiya, Common dysfunctional variants in ABCG2 are a major cause of early-onset gout, Sci Rep 3 (2013) 2014. https://doi.org/https://doi.org/10.1038/srep02014.

[18] J.A. Schulz, A.M.S. Hartz, B. Bauer, ABCB1 and ABCG2 Regulation at the Blood-Brain Barrier: Potential New Targets to Improve Brain Drug Delivery., Pharmacol Rev 75 (2023) 815–853. https://doi.org/10.1124/pharmrev.120.000025.

[19] Y. Toyoda, T. Takada, H. Suzuki, Inhibitors of Human ABCG2: From Technical Background to Recent Updates With Clinical Implications., Front Pharmacol 10 (2019) 208. https://doi.org/10.3389/fphar.2019.00208.

[20] A. Palmeira, E. Sousa, M. H. Vasconcelos, M. M. Pinto, Three Decades of P-gp Inhibitors: Skimming Through Several Generations and Scaffolds, Curr Med Chem 19 (2012) 1946–2025. https://doi.org/10.2174/092986712800167392.

[21] C.-P. Wu, S.-H. Hsiao, Y.-S. Wu, Perspectives on drug repurposing to overcome cancer multidrug resistance mediated by ABCB1 and ABCG2, Drug Resistance Updates 71 (2023) 101011. https://doi.org/10.1016/j.drup.2023.101011.

[22] A. Tamaki, C. Ierano, G. Szakacs, R.W. Robey, S.E. Bates, The controversial role of ABC transporters in clinical oncology., Essays Biochem 50 (2011) 209–32. https://doi.org/10.1042/bse0500209.

[23] L.J.A. Hardwick, S. Velamakanni, H.W. van Veen, The emerging pharmacotherapeutic significance of the breast cancer resistance protein (ABCG2), Br J Pharmacol 151 (2007) 163–174. https://doi.org/10.1038/sj.bjp.0707218.

[24] B. Stiburkova, K. Pavelcova, J. Zavada, L. Petru, P. Simek, P. Cepek, M. Pavlikova, H. Matsuo, T.R. Merriman, K. Pavelka, Functional non-synonymous variants of ABCG2 and gout risk, Rheumatology 56 (2017) 1982–1992. https://doi.org/10.1093/rheumatology/kex295.

[25] J. Xu, Y. Liu, Y. Yang, S. Bates, J.-T. Zhang, Characterization of oligomeric human half-ABC transporter ATP-binding cassette G2., J Biol Chem 279 (2004) 19781–9. https://doi.org/10.1074/jbc.M310785200.

[26] K. Wakabayashi-Nakao, A. Tamura, T. Furukawa, H. Nakagawa, T. Ishikawa, Quality control of human ABCG2 protein in the endoplasmic reticulum: ubiquitination and proteasomal degradation., Adv Drug Deliv Rev 61 (2009) 66–72. https://doi.org/10.1016/j.addr.2008.08.008.

[27] J.J. Strouse, I. Ivnitski-Steele, A. Waller, S.M. Young, D. Perez, A.M. Evangelisti, O. Ursu, C.G. Bologa, M.B. Carter, V.M. Salas, G. Tegos, R.S. Larson, T.I. Oprea, B.S. Edwards, L.A. Sklar, Fluorescent substrates for flow cytometric evaluation of efflux inhibition in ABCB1, ABCC1, and ABCG2 transporters., Anal Biochem 437 (2013) 77–87. https://doi.org/10.1016/j.ab.2013.02.018.

[28] C.W. Scharenberg, M.A. Harkey, B. Torok-Storb, The ABCG2 transporter is an efficient Hoechst 33342 efflux pump and is preferentially expressed by immature human hematopoietic progenitors., Blood 99 (2002) 507–12. https://doi.org/10.1182/blood.v99.2.507.

[29] J.E. Diestra, G.L. Scheffer, I. Català, M. Maliepaard, J.H.M. Schellens, R.J. Scheper, J.R. Germà-Lluch, M.A. Izquierdo, Frequent expression of the multi-drug resistance-associated protein BCRP/MXR/ABCP/ABCG2 in human tumours detected by the BXP-21 monoclonal antibody in paraffin-embedded material., J Pathol 198 (2002) 213–9. https://doi.org/10.1002/path.1203.

[30] N.M.I. Taylor, I. Manolaridis, S.M. Jackson, J. Kowal, H. Stahlberg, K.P. Locher, Structure of the human multidrug transporter ABCG2, Nature 546 (2017) 504–509. https://doi.org/10.1038/nature22345.

[31] O. Polgar, R.W. Robey, K. Morisaki, M. Dean, C. Michejda, Z.E. Sauna, S. V Ambudkar, N. Tarasova, S.E. Bates, Mutational analysis of ABCG2: role of the GXXXG motif., Biochemistry 43 (2004) 9448–56. https://doi.org/10.1021/bi0497953.

[32] R.W. Robey, Y. Honjo, K. Morisaki, T.A. Nadjem, S. Runge, M. Risbood, M.S. Poruchynsky, S.E. Bates, Mutations at amino-acid 482 in the ABCG2 gene affect substrate and antagonist specificity., Br J Cancer 89 (2003) 1971–8. https://doi.org/10.1038/sj.bjc.6601370.

[33] S. Macalou, R.W. Robey, G. Jabor Gozzi, S. Shukla, I. Grosjean, T. Hegedus, S. V Ambudkar, S.E. Bates, A. Di Pietro, The linker region of breast cancer resistance protein ABCG2 is critical for coupling of ATP-dependent drug transport., Cell Mol Life Sci 73 (2016) 1927–37. https://doi.org/10.1007/s00018-015-2118-5.

[34] K. Szebényi, A. Füredi, E. Bajtai, S.N. Sama, A. Csiszar, B. Gombos, P. Szabó, M. Grusch, G. Szakács, Effective targeting of breast cancer by the inhibition of P-glycoprotein mediated removal of toxic lipid peroxidation byproducts from drug tolerant persister cells., Drug Resist Updat 71 (2023) 101007. https://doi.org/10.1016/j.drup.2023.101007.

[35] J.A. Schulz, A.M.S. Hartz, B. Bauer, ABCB1 and ABCG2 Regulation at the Blood-Brain Barrier: Potential New Targets to Improve Brain Drug Delivery, Pharmacol Rev 75 (2023) 815–853. https://doi.org/10.1124/pharmrev.120.000025.

[36] E.E. Strehler, A.J. Caride, A.G. Filoteo, Y. Xiong, J.T. Penniston, A. Enyedi, Plasma membrane Ca2+ ATPases as dynamic regulators of cellular calcium handling., Ann N Y Acad Sci 1099 (2007) 226–36. https://doi.org/10.1196/annals.1387.023.

[37] E. Strehler, M. Treiman, Calcium Pumps of Plasma Membrane and Cell Interior, Curr Mol Med 4 (2004) 323–335. https://doi.org/10.2174/1566524043360735.

[38] K.D. Osborn, A. Zaidi, A. Mandal, R.J.B. Urbauer, C.K. Johnson, Single-Molecule Dynamics of the Calcium-Dependent Activation of Plasma-Membrane Ca2+-ATPase by Calmodulin, Biophys J 87 (2004) 1892–1899. https://doi.org/10.1529/biophysj.103.039404.

[39] C. Timmann, T. Thye, M. Vens, J. Evans, J. May, C. Ehmen, J. Sievertsen, B. Muntau, G. Ruge, W. Loag, D. Ansong, S. Antwi, E. Asafo-Adjei, S.B. Nguah,

K.O. Kwakye, A.O.Y. Akoto, J. Sylverken, M. Brendel, K. Schuldt, C. Loley, A. Franke, C.G. Meyer, T. Agbenyega, A. Ziegler, R.D. Horstmann, Genome-wide association study indicates two novel resistance loci for severe malaria., Nature 489 (2012) 443–446. https://doi.org/10.1038/nature11334.

[40]   G. Bedu-Addo, S. Meese, F.P. Mockenhaupt, An ATP2B4 polymorphism protects against malaria in pregnancy., J Infect Dis 207 (2013) 1600–1603. https://doi.org/10.1093/infdis/jit070.

[41]   B. Zámbó, G. Várady, R. Padányi, E. Szabó, A. Németh, T. Langó, Á. Enyedi, B. Sarkadi, Decreased calcium pump expression in human erythrocytes is connected to a minor haplotype in the ATP2B4 gene, Cell Calcium 65 (2017) 73–79. https://doi.org/10.1016/j.ceca.2017.02.001.

[42]   F. Joof, E. Hartmann, A. Jarvis, A. Colley, J.H. Cross, M. Avril, A.M. Prentice, C. Cerami, Genetic variations in human ATP2B4 gene alter Plasmodium falciparum in vitro growth in RBCs from Gambian adults, Malar J 22 (2023) 5. https://doi.org/10.1186/s12936-022-04359-4.

[43]   F. Joof, E. Hartmann, A. Jarvis, A. Colley, J.H. Cross, M. Avril, A.M. Prentice, C. Cerami, Genetic variations in human ATP2B4 gene alter Plasmodium falciparum in vitro growth in RBCs from Gambian adults, Malar J 22 (2023) 5. https://doi.org/10.1186/s12936-022-04359-4.

[44]   M. Adjemout, B. Pouvelle, F. Thiam, A. Thiam, M. Torres, S. Nisar, B. Mbengue, A. Dieye, P. Rihet, S. Marquet, Concurrent PIEZO1 activation and ATP2B4 blockade effectively reduce the risk of cerebral malaria and inhibit in vitro Plasmodium falciparum multiplication in red blood cells., Genes Dis 10 (2023) 2210–2214. https://doi.org/10.1016/j.gendis.2023.02.029.

[45]   R. Ferreira, K. Ohneda, M. Yamamoto, S. Philipsen, GATA1 function, a paradigm for transcription factors in hematopoiesis., Mol Cell Biol 25 (2005) 1215–27. https://doi.org/10.1128/MCB.25.4.1215-1227.2005.

[46]   E.N. Stern, S. Lessard, P.G. Schupp, F. Sher, G. Lettre, D.E. Bauer, An Essential Erythroid-Specific Enhancer of ATP2B4 Associated with Red Blood Cell Traits and Malaria Susceptibility, Blood 128 (2016) 1250–1250. https://doi.org/10.1182/blood.V128.22.1250.1250.

[47] C.B. Jackson, M. Farzan, B. Chen, H. Choe, Mechanisms of SARS-CoV-2 entry into cells, Nat Rev Mol Cell Biol 23 (2022) 3–20. https://doi.org/10.1038/s41580-021-00418-x.

[48] J. Zhang, T. Xiao, Y. Cai, B. Chen, Structure of SARS-CoV-2 spike protein., Curr Opin Virol 50 (2021) 173–182. https://doi.org/10.1016/j.coviro.2021.08.010.

[49] O.C. Grant, D. Montgomery, K. Ito, R.J. Woods, Analysis of the SARS-CoV-2 spike protein glycan shield reveals implications for immune recognition, Sci Rep 10 (2020) 14991. https://doi.org/10.1038/s41598-020-71748-7.

[50] J.D. Marth, P.K. Grewal, Mammalian glycosylation in immunity, Nat Rev Immunol 8 (2008) 874–887. https://doi.org/10.1038/nri2417.

[51] E. Taka, S.Z. Yilmaz, M. Golcuk, C. Kilinc, U. Aktas, A. Yildiz, M. Gur, Critical Interactions Between the SARS-CoV-2 Spike Glycoprotein and the Human ACE2 Receptor, J Phys Chem B 125 (2021) 5537–5548. https://doi.org/10.1021/acs.jpcb.1c02048.

[52] R.J. Parsons, P. Acharya, Evolution of the SARS-CoV-2 Omicron spike., Cell Rep 42 (2023) 113444. https://doi.org/10.1016/j.celrep.2023.113444.

[53] V. Hall, S. Foulkes, F. Insalata, P. Kirwan, A. Saei, A. Atti, E. Wellington, J. Khawam, K. Munro, M. Cole, C. Tranquillini, A. Taylor-Kerr, N. Hettiarachchi, D. Calbraith, N. Sajedi, I. Milligan, Y. Themistocleous, D. Corrigan, L. Cromey, L. Price, S. Stewart, E. de Lacy, C. Norman, E. Linley, A.D. Otter, A. Semper, J. Hewson, S. D'Arcangelo, M. Chand, C.S. Brown, T. Brooks, J. Islam, A. Charlett, S. Hopkins, Protection against SARS-CoV-2 after Covid-19 Vaccination and Previous Infection, New England Journal of Medicine 386 (2022) 1207–1220. https://doi.org/10.1056/NEJMoa2118691.

[54] N. Kojima, J.D. Klausner, Protective immunity after recovery from SARS-CoV-2 infection., Lancet Infect Dis 22 (2022) 12–14. https://doi.org/10.1016/S1473-3099(21)00676-9.

[55] D.S. Khoury, D. Cromer, A. Reynaldi, T.E. Schlub, A.K. Wheatley, J.A. Juno, K. Subbarao, S.J. Kent, J.A. Triccas, M.P. Davenport, Neutralizing antibody levels are highly predictive of immune protection from symptomatic SARS-CoV-2 infection, Nat Med 27 (2021) 1205–1211. https://doi.org/10.1038/s41591-021-01377-8.

[56] L. Renia, L.F. Ng, Acquired immunity against SARS-CoV-2 infection and vaccination, EMBO Mol Med 15 (2023). https://doi.org/10.15252/emmm.202216345.

[57] L. Jaki, S. Weigang, L. Kern, S. Kramme, A.G. Wrobel, A.B. Grawitz, P. Nawrath, S.R. Martin, T. Dähne, J. Beer, M. Disch, P. Kolb, L. Gutbrod, S. Reuter, K. Warnatz, M. Schwemmle, S.J. Gamblin, E. Neumann-Haefelin, D. Schnepf, T. Welte, G. Kochs, D. Huzly, M. Panning, J. Fuchs, Total escape of SARS-CoV-2 from dual monoclonal antibody therapy in an immunocompromised patient, Nat Commun 14 (2023) 1999. https://doi.org/10.1038/s41467-023-37591-w.

[58] J. Miller, N.P. Hachmann, A.Y. Collier, N. Lasrado, C.R. Mazurek, R.C. Patio, O. Powers, N. Surve, J. Theiler, B. Korber, D.H. Barouch, Substantial Neutralization Escape by SARS-CoV-2 Omicron Variants BQ.1.1 and XBB.1, New England Journal of Medicine 388 (2023). https://doi.org/10.1056/nejmc2214314.

[59] E.J. Wherry, D.H. Barouch, T cell immunity to COVID-19 vaccines, Science (1979) 377 (2022) 821–822. https://doi.org/10.1126/science.add2897.

[60] P. Moss, The T cell immune response against SARS-CoV-2, Nat Immunol 23 (2022) 186–193. https://doi.org/10.1038/s41590-021-01122-w.

[61] F. Amanat, D. Stadlbauer, S. Strohmeier, T.H.O. Nguyen, V. Chromikova, M. McMahon, K. Jiang, G.A. Arunkumar, D. Jurczyszak, J. Polanco, M. Bermudez-Gonzalez, G. Kleiner, T. Aydillo, L. Miorin, D.S. Fierer, L.A. Lugo, E.M. Kojic, J. Stoever, S.T.H. Liu, C. Cunningham-Rundles, P.L. Felgner, T. Moran, A. García-Sastre, D. Caplivski, A.C. Cheng, K. Kedzierska, O. Vapalahti, J.M. Hepojoki, V. Simon, F. Krammer, A serological assay to detect SARS-CoV-2 seroconversion in humans., Nat Med 26 (2020) 1033–1036. https://doi.org/10.1038/s41591-020-0913-5.

[62] L. Mátés, M.K.L. Chuah, E. Belay, B. Jerchow, N. Manoj, A. Acosta-Sanchez, D.P. Grzela, A. Schmitt, K. Becker, J. Matrai, L. Ma, E. Samara-Kuko, C. Gysemans, D. Pryputniewicz, C. Miskey, B. Fletcher, T. VandenDriessche, Z. Ivics, Z. Izsvák, Molecular evolution of a novel hyperactive Sleeping Beauty transposase enables robust stable gene transfer in vertebrates, Nat Genet 41 (2009) 753–761. https://doi.org/10.1038/ng.343.

[63] Z. Bartos, L. Homolya, Identification of Specific Trafficking Defects of Naturally Occurring Variants of the Human ABCG2 Transporter, Front Cell Dev Biol 9 (2021). https://doi.org/10.3389/fcell.2021.615729.

[64] O. Mózner, B. Zámbó, B. Sarkadi, Modulation of the Human Erythroid Plasma Membrane Calcium Pump (PMCA4b) Expression by Polymorphic Genetic Variants., Membranes (Basel) 11 (2021). https://doi.org/10.3390/membranes11080586.

[65] L. Homolya, M. Holló, M. Müller, E.B. Mechetner, B. Sarkadi, A new method for a quantitative assessment of P-glycoprotein-related multidrug resistance in tumour cells., Br J Cancer 73 (1996) 849–55. https://doi.org/10.1038/bjc.1996.151.

[66] G. Boncompain, S. Divoux, N. Gareil, H. de Forges, A. Lescure, L. Latreche, V. Mercanti, F. Jollivet, G. Raposo, F. Perez, Synchronization of secretory protein traffic in populations of cells, Nat Methods 9 (2012) 493–498. https://doi.org/10.1038/nmeth.1928.

[67] C. Özvegy-Laczka, G. Várady, G. Köblös, O. Ujhelly, J. Cervenak, J.D. Schuetz, B.P. Sorrentino, G.J. Koomen, A. Váradi, K. Német, B. Sarkadi, Function-dependent conformational changes of the ABCG2 multidrug transporter modify its interaction with a monoclonal antibody on the cell surface, Journal of Biological Chemistry 280 (2005) 4219–4227. https://doi.org/10.1074/jbc.M411338200.

[68] O. Mózner, B. Zámbó, Z. Bartos, A. Gergely, K.S. Szabó, B. Jezsó, Á. Telbisz, G. Várady, L. Homolya, T. Hegedűs, B. Sarkadi, Expression, Function and Trafficking of the Human ABCG2 Multidrug Transporter Containing Mutations in an Unstructured Cytoplasmic Loop, Membranes (Basel) 13 (2023) 822. https://doi.org/10.3390/MEMBRANES13100822/S1.

[69] K. Natarajan, J. Bhullar, S. Shukla, M. Burcu, Z.-S. Chen, S. V. Ambudkar, M.R. Baer, The Pim kinase inhibitor SGI-1776 decreases cell surface expression of P-glycoprotein (ABCB1) and breast cancer resistance protein (ABCG2) and drug transport Pim-1 dependent and -independent mechanisms, Biochem Pharmacol 85 (2013) 1–22. https://doi.org/10.1016/j.bcp.2012.12.006.

[70] Y. Xie, K. Xu, D.E. Linn, X. Yang, Z. Guo, H. Shimelis, T. Nakanishi, D.D. Ross, H. Chen, L. Fazli, M.E. Gleave, Y. Qiu, The 44-kDa Pim-1 kinase phosphorylates BCRP/ABCG2 and thereby promotes its multimerization and drug-resistant

activity in human prostate cancer cells, Journal of Biological Chemistry 283 (2008) 3349–3356. https://doi.org/10.1074/jbc.M707773200.

[71] O.M. Woodward, D.N. Tukaye, J. Cui, P. Greenwell, L.M. Constantoulakis, B.S. Parker, A. Rao, M. Kottgen, P.C. Maloney, W.B. Guggino, M. Köttgen, P.C. Maloney, W.B. Guggino, Gout-causing Q141K mutation in ABCG2 leads to instability of the nucleotide-binding domain and can be corrected with small molecules, Proceedings of the National Academy of Sciences 110 (2013) 5223–5228. https://doi.org/10.1073/pnas.1214530110.

[72] T. Furukawa, K. Wakabayashi, A. Tamura, H. Nakagawa, Y. Morishima, Y. Osawa, T. Ishikawa, Major SNP (Q141K) variant of human ABC transporter ABCG2 undergoes lysosomal and proteasomal degradations., Pharm Res 26 (2009) 469–79. https://doi.org/10.1007/s11095-008-9752-7.

[73] M. Stornaiuolo, L. V Lotti, N. Borgese, M.-R. Torrisi, G. Mottola, G. Martire, S. Bonatti, KDEL and KKXX retrieval signals appended to the same reporter protein determine different trafficking between endoplasmic reticulum, intermediate compartment, and Golgi complex., Mol Biol Cell 14 (2003) 889–902. https://doi.org/10.1091/mbc.e02-08-0468.

[74] J. Shin, R.L. Dunbrack, S. Lee, J.L. Strominger, Signals for retention of transmembrane proteins in the endoplasmic reticulum studied with CD4 truncation mutants., Proc Natl Acad Sci U S A 88 (1991) 1918–22. https://doi.org/10.1073/pnas.88.5.1918.

[75] M. Huls, C.D.A. Brown, A.S. Windass, R. Sayer, J.J.M.W. van den Heuvel, S. Heemskerk, F.G.M. Russel, R. Masereeuw, The breast cancer resistance protein transporter ABCG2 is expressed in the human kidney proximal tubule apical membrane., Kidney Int 73 (2008) 220–5. https://doi.org/10.1038/sj.ki.5002645.

[76] B. Zámbó, O. Mózner, Z. Bartos, G. Török, G. Várady, Á. Telbisz, L. Homolya, T.I. Orbán, B. Sarkadi, Cellular expression and function of naturally occurring variants of the human ABCG2 multidrug transporter., Cell Mol Life Sci 77 (2020) 365–378. https://doi.org/10.1007/s00018-019-03186-2.

[77] H. Peng, J. Qi, Z. Dong, J.-T. Zhang, Dynamic vs static ABCG2 inhibitors to sensitize drug resistant cancer cells., PLoS One 5 (2010) e15276. https://doi.org/10.1371/journal.pone.0015276.

[78] G. Boncompain, F. Perez, Synchronizing Protein Transport in the Secretory Pathway, Curr Protoc Cell Biol 57 (2012). https://doi.org/10.1002/0471143030.cb1519s57.

[79] T.I. Orbán, L. Seres, C. Özvegy-Laczka, N.B. Elkind, B. Sarkadi, L. Homolya, Combined localization and real-time functional studies using a GFP-tagged ABCG2 multidrug transporter, Biochem Biophys Res Commun 367 (2008) 667–673. https://doi.org/10.1016/j.bbrc.2007.12.172.

[80] S. Lessard, E.S. Gatof, M. Beaudoin, P.G. Schupp, F. Sher, A. Ali, S. Prehar, R. Kurita, Y. Nakamura, E. Baena, J. Ledoux, D. Oceandy, D.E. Bauer, G. Lettre, An erythroid-specific ATP2B4 enhancer mediates red blood cell hydration and malaria susceptibility, Journal of Clinical Investigation 127 (2017) 3065–3074. https://doi.org/10.1172/JCI94378.

[81] D. Farré, R. Roset, M. Huerta, J.E. Adsuara, L. Roselló, M.M. Albà, X. Messeguer, Identification of patterns in biological sequences at the ALGGEN server: PROMO and MALGEN., Nucleic Acids Res 31 (2003) 3651–3653. https://doi.org/10.1093/nar/gkg605.

[82] O. Mózner, J. Moldvay, K.S. Szabó, D. Vaskó, J. Domján, D. Ács, Z. Ligeti, C. Fehér, E. Hirsch, L. Puskás, C. Stahl, M. Frey, B. Sarkadi, Application of a Receptor-Binding-Domain-Based Simple Immunoassay for Assessing Humoral Immunity against Emerging SARS-CoV-2 Virus Variants, Biomedicines 11 (2023) 3193. https://doi.org/10.3390/BIOMEDICINES11123193/S1.

[83] O. Mózner, B. Zámbó, Z. Bartos, A. Gergely, K.S. Szabó, B. Jezsó, Á. Telbisz, G. Várady, L. Homolya, T. Hegedűs, B. Sarkadi, Expression, Function and Trafficking of the Human ABCG2 Multidrug Transporter Containing Mutations in an Unstructured Cytoplasmic Loop, Membranes (Basel) 13 (2023) 822. https://doi.org/10.3390/membranes13100822.

[84] D.M. Langhi, J.O. Bordin, Duffy blood group and malaria., Hematology 11 (2006) 389–98. https://doi.org/10.1080/10245330500469841.

[85] C. Tournamille, Y. Colin, J.P. Cartron, C. Le Van Kim, Disruption of a GATA motif in the Duffy gene promoter abolishes erythroid gene expression in Duffy-negative individuals., Nat Genet 10 (1995) 224–228. https://doi.org/10.1038/ng0695-224.

[86] A. Villegas-Mendez, N. Stafford, M.J. Haley, N.E. Pravitasari, F. Baudoin, A. Ali, P.B.S. Asih, J.E. Siregar, E. Baena, D. Syafruddin, K.N. Couper, D. Oceandy, The plasma membrane calcium ATPase 4 does not influence parasite levels but partially promotes experimental cerebral malaria during murine blood stage malaria., Malar J 20 (2021) 297. https://doi.org/10.1186/s12936-021-03832-w.

[87] Y. Huang, C. Yang, X. Xu, W. Xu, S. Liu, Structural and functional properties of SARS-CoV-2 spike protein: potential antivirus drug development for COVID-19, Acta Pharmacol Sin 41 (2020) 1141–1149. https://doi.org/10.1038/s41401-020-0485-4.

[88] L. Du, Y. He, Y. Zhou, S. Liu, B.-J. Zheng, S. Jiang, The spike protein of SARS-CoV — a target for vaccine and therapeutic development, Nat Rev Microbiol 7 (2009) 226–236. https://doi.org/10.1038/nrmicro2090.

[89] M. Manak, L. Gagnon, S. Phay-Tran, P. Levesque-Damphousse, A. Fabie, M. Daugan, S.T. Khan, P. Proud, B. Hussey, D. Knott, S. Charlton, B. Hallis, G.R. Medigeshi, N. Garg, A. Anantharaj, R. Raqib, P. Sarker, M.M. Alam, M. Rahman, M. Murreddu, A. Balgobind, R. Hofman, S. Grappi, R. Coluccio, P. Calandro, E. Montomoli, G. Mattiuzzo, S. Prior, Y. Le Duff, M. Page, J. Mitchell, L.M. Schwartz, Y.C. Bartsch, A. Azizi, V. Bernasconi, V. Zala, A.P. De Almeida, H. Fassoulas, T. Agrawal, J. Singh, A.K. Roy, S. Berndsen, M. de Mooij, H. Buitendijk, C. Stalpers, M. Jarju, F. Battistella, R. Jeeninga, D. Duijsings, I. Razzano, E. Molesti, L. Mazzini, A. Boccuto, A. Holder, E. Mee, M. Hurley, J. Padley, N. Rose, T. Gorman, J. Vila-Belda, H. James, J. Carless, Standardised quantitative assays for anti-SARS-CoV-2 immune response used in vaccine clinical trials by the CEPI Centralized Laboratory Network: a qualification analysis, Lancet Microbe 5 (2024) e216–e225. https://doi.org/10.1016/S2666-5247(23)00324-5.

[90] H. Papp, E. Tóth, J. Bóvári-Biri, K. Bánfai, P. Juhász, M. Mahdi, L.C. Russo, D. Bajusz, A. Sipos, L. Petri, T.V. Szalai, Á. Kemény, M. Madai, A. Kuczmog, G. Batta, O. Mózner, D. Vaskó, E. Hirsch, P. Bohus, G. Méhes, J. Tőzsér, N.J. Curtin, Z. Helyes, A. Tóth, N.C. Hoch, F. Jakab, G.M. Keserű, J.E. Pongrácz, P. Bai, The PARP inhibitor rucaparib blocks SARS-CoV-2 virus binding to cells and the

immune reaction in models of COVID-19, Br J Pharmacol (2024). https://doi.org/10.1111/bph.17305.

[91] D. Vaskó, E. Pantea, J. Domján, C. Fehér, O. Mózner, B. Sarkadi, Z.K. Nagy, G.J. Marosi, E. Hirsch, Raman and NIR spectroscopy-based real-time monitoring of the membrane filtration process of a recombinant protein for the diagnosis of SARS-CoV-2, Int J Pharm 660 (2024). https://doi.org/10.1016/j.ijpharm.2024.124251.

9   Bibliography of the publications

Publications discussed in the dissertation

Mózner, Orsolya ; Zámbó, Boglárka ; Bartos, Zsuzsa ; Gergely, Anna ; Szabó, Kata Sára ; Jezsó, Bálint ; Telbisz, Ágnes ; Várady, György ; Homolya, László ; Hegedűs, Tamás ; Balázs Sarkadi
Expression, Function and Trafficking of the Human ABCG2 Multidrug Transporter Containing Mutations in an Unstructured Cytoplasmic Loop
MEMBRANES (BASEL) 13 : 10 Paper: 822 , 14 p. (2023)
IF: 3.3
DOI: 10.3390/membranes13100822

Mózner, Orsolya* ; Zámbó, Boglárka*; Sarkadi, Balázs
Modulation of the Human Erythroid Plasma Membrane Calcium Pump (PMCA4b) Expression by Polymorphic Genetic Variants
MEMBRANES (BASEL) 11 : 8 Paper: 586 , 10 p. (2021)
IF: 4.562
DOI: 10.3390/membranes11080586

Mózner, Orsolya ; Moldvay, Judit ; Szabó, Kata Sára ; Vaskó, Drorttya ; Domján, Júlia ; Ács, Dorottya ; Ligeti, Zoltán ; Fehér, Csaba ; Hirsch, Edit ; Puskás, László ; Stahl, Cordula ; Frey, Manfred ; Sarkadi, Balázs
Application of a Receptor-Binding-Domain-Based Simple Immunoassay for Assessing Humoral Immunity against Emerging SARS-CoV-2 Virus Variants
BIOMEDICINES 11 : 12 Paper: 3193 , 10 p. (2023)
IF: 3.9
DOI: 10.3390/biomedicines11123193

Publications not discussed in the dissertation

Papp H, Tóth E, Bóvári-Biri J, Bánfai K, Juhász P, Mahdi M, Russo LC, Bajusz D, Sipos A, Petri L, Szalai TV, Kemény Á, Madai M, Kuczmog A, Batta Gy, **Mózner O**, Vaskó D, Hirsch E, Bohus P, Méhes G, Tőzsér J, Curtin NJ, Helyes Zs, Tóth A, Hoch NC, Jakab F, Keserű GYM, Pongrácz JE, Bai P
The PARP inhibitor rucaparib blocks SARS-CoV-2 virus binding to cells and the immune reaction in models of COVID-19
BRITISH JOURNAL OF PHARMACOLOGY

IF: 6,8# (predicted)

DOI: 10.1111/bph.17305, 22 p. (2024)

Vaskó, Dorottya ; Pantea, Eszter ; Domján, Júlia ; Fehér, Csaba ; **Mózner, Orsolya** ; Sarkadi, Balázs ; Nagy, Zsombor; Marosi, György J. ; Hirsch, Edit
Raman and NIR spectroscopy-based real-time monitoring of the membrane filtration process of a recombinant protein for the diagnosis of SARS-CoV-2

INTERNATIONAL JOURNAL OF PHARMACEUTICS 660 Paper: 124251 , 10 p. (2024)
IF: 5,3# (predicted)
DOI: 10.1016/j.ijpharm.2024.124251

Broca-Brisson, Léa ; Harati, Rania ; Disdier, Clémence ; **Mozner, Orsolya** ; Gaston-Breton, Romane ; Maïza, Auriane ; Costa, Narciso ; Guyot, Anne-Cécile ; Sarkadi, Balazs ; Apati, Agota ; Skelton, Matthew R ; Madrange, Lucie ; Yates, Frank ; Armengaud, Jean ; Hamoudi, Rifat ; Mabondzo, Aloise
Deciphering neuronal deficit and protein profile changes in human brain organoids from patients with creatine transporter
deficiency
ELIFE 12 Paper: RP88459 , 22 p. (2023)
IF: 6,4
DOI: 10.7554/eLife.88459

Pálinkás, M. ; Szabó, E. ; Kulin, A. ; **Mózner, O.** ; Rásonyi, R. ; Juhász, P. ; Nagy, K. ; Várady, G. ; Vörös, D. ; Zámbó, B. ; Sarkadi, B. ; Poór, Gy.
Genetic polymorphisms and decreased protein expression of ABCG2 urate transporters are associated with susceptibility to gout, disease severity and renal-overload hyperuricemia
CLINICAL AND EXPERIMENTAL MEDICINE 23 pp. 1277-1284. , 8 p. (2023)
IF: 3,2
DOI: 10.1007/s10238-022-00848-7

Szabó, Edit ; Kulin, Anna ; **Mózner, Orsolya** ; Korányi, László ; Literáti-Nagy, Botond ; Vitai, Márta ; Cserepes, Judit; Sarkadi, Balázs ; Várady, György
Potential role of the ABCG2-Q141K polymorphism in type 2 diabetes
PLOS ONE 16 : 12 Paper: e0260957 , 9 p. (2021)
IF: 3,752
DOI: 10.1371/journal.pone.0260957

Telbisz, Ágnes ; Ambrus, Csilla* ; **Mózner, Orsolya** ; Szabó, Edit ; Várady, György ; Bakos, Éva ; Sarkadi, Balázs ; Özvegy-Laczka, Csilla
Interactions of Potential Anti-COVID-19 Compounds with Multispecific ABC and OATP Drug Transporters
PHARMACEUTICS 13 : 1 Paper: 81 , 18 p. (2021)
IF: 6,525
DOI: 10.3390/pharmaceutics13010081

Zámbó, B. ; **Mózner, O.*** ; Bartos, Z. ; Török, G. ; Várady, G. ; Telbisz, Á. ; Homolya, L. ; Orbán, T.I. ; Sarkadi, B.
Cellular expression and function of naturally occurring variants of the human ABCG2 multidrug transporter
CELLULAR AND MOLECULAR LIFE SCIENCES 77 : 2 pp. 365-378. , 14 p. (2020)
IF: 9,261
DOI: 10.1007/s00018-019-03186-2

Zámbó, B ; Bartos, Z ; **Mózner, O** ; Szabó, E ; Várady, G ; Poór, G ; Pálinkás, M ;
Andrikovics, H ; Hegedűs, T ; Homolya, L ; Sarkadi, B
Clinically relevant mutations in the ABCG2 transporter uncovered by genetic analysis
linked to erythrocyte membrane protein
Expression
SCIENTIFIC REPORTS 10;8(1):7487. (2018)
IF: 4,011
DOI: 10.1038/s41598-018-25695-z

10 Acknowledgements

I would like to thank my supervisor, Dr. Balázs Sarkadi, for his exceptional mentorship throughout my BSc, MSc and PhD studies. His guidance and encouragement have played a significant role in my academic and personal development, and his support at every step has been invaluable in motivating me to pursue a career in science.

I would like to thank my research advisor, Dr. Homolya László for his support throughout my PhD research and under the Cooperative Doctoral Program.

I am grateful to my colleagues and co-authors at the Research Centre for Natural Sciences for ensuring a great community, and for our collaboration on interesting projects. I would like to give special thanks to Dr. Zsuzsa Bartos, Dr. Ágnes Telbisz, Dr. Ágota Apáti, Dr. György Várady, Dr. Edit Szabó, Anna Kulin, Dr. Csilla Laczka, Dr. György Török, Dr. Éva Bakos, Dr. Zoltán Ligeti, Dr. Tamás Orbán, Dr. Tamás Hegedűs, Dr. Bálint Jezsó for our collaboration and their support throughout my PhD studies. I am very thankful to Dr. Boglárka Zámbó for her patient mentoring during my BSc and MSc studies and our ongoing collaboration.

I would like to thank Dr. Beáta Vértessy for her support throughout my university and PhD studies as my advisor and university supervisor.

I am very thankful for Dr. Szilárd Tóth reading and revising the dissertation as my in-house opponent at the Research Centre for Natural Sciences.

I would like to thank official opponents Dr. Viola Pomozi and Dr. Balázs Enyedi for their thorough review of my thesis.

I would like to thank all my colleagues, friends, and the Biomembrane community in the Research Centre for Natural Sciences for their support. I would like to give special thanks to Dr. Orsolya Kolacsek, Dr. Luca Gál, Dr. Julianna Lilienberg, Kata Sára Szabó, Kornélia Némethy, Gyöngyi Bézsenyi and Kata Rieth for their support.

I would like to thank Dr. Judit Moldvay, Dr. Edit Buzás, and Dr. András Falus for their guidance, encouragement and belief in our shared efforts to advance diagnostic solutions.

I am very thankful to my host professors, Dr. Susan Bates and Dr. Tito Fojo, as well as their colleagues Dr. Maryam Safari, Dr. Luigi Scotto and Dr. Ping Zhou at Columbia University, for their kindness and warm welcome during my visiting student researcher period in their laboratory.

I would like to thank colleagues Dr. Edit Hirsch and Dr. Csaba Fehér at the Budapest University of Technology and Economics for our collaboration on the RBD protein production.

I would like to thank my friends and my family—my parents, my brother, and my husband, Péter Tőke—for their unwavering support and encouragement.